RADIATION RESEARCH 176, 678–687 (2011)
0033-7587/11 $15.00

DOI: 10.1667/RR2631.1

Associations of Ionizing Radiation and Breast Cancer-Related Serum Hormone and Growth Factor Levels in Cancer-Free Female A-Bomb Survivors

Eric J. Grant,[a,1] Kazuo Neriishi,[b] John Cologne,[c] Hidetaka Eguchi,[d] Tomonori Hayashi,[e] Susan Geyer,[f] Shizue Izumi,[g] Nobuo Nishi,[h] Charles Land,[i] Richard G. Stevens,[j] Gerald B. Sharp[k] and Kei Nakachi[e]

[a] *Department of Epidemiology,* [b] *Department of Clinical Studies,* [c] *Department of Statistics, and* [e] *Department of Radiobiology/Molecular Epidemiology, Radiation Effects Research Foundation, 5-2 Hijiyama Park, Minamiku, Hiroshima 732-0815, Japan;* [d] *Translational Research Center, International Medical Center, Saitama Medical University, 1397-1 Yamane, Hidaka-shi, Saitama 350-1241, Japan;* [f] *Department of Internal Medicine, The Ohio State University, Columbus, Ohio 43210;* [g] *Department of Computer Science and Intelligent Systems, Oita University, 700 Dannoharu, Oita, 870-1192 Japan;* [h] *Center for Collaboration and Partnership, National Institute of Health and Nutrition, 1-23-1 Toyama, Shinjuku-ku, Tokyo 162-8636, Japan;* [i] *Radiation Epidemiology Branch, National Cancer Institute, Bethesda, Maryland 20892-7335;* [j] *Department of Community Medicine, University of Connecticut Health Center, Connecticut 06030; and* [k] *Epidemiology Branch, Basic Sciences Program, Division of AIDS, National Institute of Allergy and Infectious Diseases, National Institutes of Health, Bethesda, Maryland 20892*

Grant, E. J., Neriishi, K., Cologne, J., Eguchi, H., Hayashi, T., Geyer, S., Izumi, S., Nishi, N., Land, C., Stevens, R. G., Sharp, G. B. and Nakachi, K. Associations of Ionizing Radiation and Breast Cancer-Related Serum Hormone and Growth Factor Levels in Cancer-Free Female A-Bomb Survivors. *Radiat. Res.* 176, 678–687 (2011).

Levels of exposure to ionizing radiation are increasing for women worldwide due to the widespread use of CT and other radiologic diagnostic modalities. Exposure to ionizing radiation as well as increased levels of estradiol and other sex hormones are acknowledged breast cancer risk factors, but the effects of whole-body radiation on serum hormone levels in cancer-free women are unknown. This study examined whether ionizing radiation exposure is associated with levels of serum hormones and other markers that may mediate radiation-associated breast cancer risk. Serum samples were measured from cancer-free women who attended biennial health examinations with a wide range of past radiation exposure levels ($N = 412$, ages 26–79). The women were selected as controls for separate case-control studies from a cohort of A-bomb survivors. Outcome measures included serum levels of total estradiol, bioavailable estradiol, testosterone, progesterone, prolactin, insulin-like growth factor-1 (IGF1), insulin-like growth factor-binding protein 3 (IGFBP-3), and ferritin. Relationships were assessed using repeated-measures regression models fitted with generalized estimating equations. Geometric mean serum levels of total estradiol and bioavailable estradiol increased with 1 Gy of radiation dose among samples collected from postmenopausal women (17%$_{1Gy}$, 95% CI: 1%–36% and 21%$_{1Gy}$, 95% CI: 4%–40%, respectively), while they decreased in samples collected from premenopausal women (−11%$_{1Gy}$, 95% CI: −20%–1% and −12%$_{1Gy}$, 95% CI: −20%– −2%, respectively). Interactions by menopausal status were significant ($P = 0.003$ and $P < 0.001$, respectively). Testosterone levels increased with radiation dose in postmenopausal samples (30.0%$_{1Gy}$, 95% CI: 13%–49%) while they marginally decreased in premenopausal samples (−10%$_{1Gy}$, 95% CI: −19%–0%) and the interaction by menopausal status was significant ($P < 0.001$). Serum levels of IGF1 increased linearly with radiation dose (11%$_{1Gy}$, 95% CI: 2%–18%) and there was a significant interaction by menopausal status ($P = 0.014$). Radiation-associated changes in serum levels of estradiol, bioavailable estradiol, testosterone and IGF1 were modified by menopausal status at the time of collection. No associations with radiation were observed in serum levels of progesterone, prolactin, IGFBP-3 or ferritin. © 2011 by Radiation Research Society

INTRODUCTION

Exposure to ionizing radiation via diagnostic imaging, particularly CT scans, continues to increase worldwide (*1*). Numerous studies have proven the association between exposure to ionizing radiation and breast cancer (*2*). Moreover, data from the A-bomb survivors indicate that the breast is particularly susceptible to ionizing radiation exposure, with an attributable fraction for breast cancer of 27% for all women exposed to more than 5 mGy (*3*) [a radiation dose roughly twice the yearly background dose (*4*)]. Breast cancer has also been associated with levels of endogenous hormones, particularly estradiol (E_2) (*5–7*). Estrogens stimulate cell proliferation (*8*) and possibly exert a direct genotoxic effect on breast epithelial cells (*9*).

Other circulating hormones and proteins, including non-sex hormone-binding globulin (SHBG)-bound

Note. The online version of this article (DOI: 10.1667/RR2631.1) contains supplementary information that is available to all authorized users.

[1] Address for correspondence: Department of Epidemiology, Radiation Effects Research Foundation, 5-2 Hijiyama Park, Minami-ku, Hiroshima 732-0815, Japan; e-mail: egrant@rerf.or.jp.

estradiol, testosterone (*7*) and insulin-like growth factor 1 (IGF1), have been associated with breast cancer (*10*). Additional serum markers have been hypothesized to be associated with breast cancer, including IGFBP-3 (*11*), progesterone (*12*), prolactin (*13*) and ferritin. Ferritin levels and ionizing radiation are associated with increased levels of free radicals, and high ferritin levels have been reported to result in cell transformation and immortalization in mammary glands (*14*).

The question of whether ionizing radiation exposure modifies the underlying levels of risk-related circulating markers has not been addressed, however, and could be important in mechanistic studies of breast cancer or other hormone-related cancers after ionizing radiation exposure. The primary purpose of this project is to examine whether serum levels of risk-related markers vary with past radiation exposure in a representative sample of cancer-free female A-bomb survivors.

MATERIALS AND METHODS

Subjects

Study subjects were selected from the Adult Health Study (AHS), a longitudinal cohort study of A-bomb survivors initiated in 1958 (*15*). The AHS features biennial clinical examinations with serum collection and well-characterized radiation doses for numerous body organs (*16*). Serum samples were selected in the context of concurrent case-control studies wherein controls were selected by incidence density sampling from all subjects who met eligibility requirements and were at risk for a first primary cancer of any type at the time an index case was diagnosed. Eligibility was defined as women who were free from various medical conditions (oophorectomy, current exogenous hormone treatment, prior malignancies, pregnant), were cancer-free for at least 2 years after serum collection, and had estimated radiation organ doses. Hormone-related diseases/conditions were based on self-reports or, in the case of extreme measured values, a medical chart review. Samples were matched to an index case on age at collection (±2 years), sample collection year (same decade), city (Hiroshima or Nagasaki), and counter-matched using breast radiation dose strata (low, medium and high with cut-points at 5 mGy and 790 mGy) (*17*). Counter-matching assures a wide exposure range while still providing an appropriate sample for inference of the exposure effects within the underlying cancer-free cohort (*18*). Because it is not known which organ system might be responsible for changes to serum markers, we used doses to the colon for purposes of analyses. The colon is a centrally located organ, and colon doses have been used as representative doses in other studies (e.g. for overall solid cancer risk estimates), although the results should be relatively insensitive to the organ chosen since the doses to all organs are highly correlated. Radiation doses to the colon were adjusted to account for random errors in the individual radiation dose estimates (*19*). Menopausal status at the time of sample collection was assigned using a two-step process. First, we used a conservative age range to assign menopausal status. If a woman was less than 43 years of age at the time of sample collection, she was designated premenopausal (N = 218); if she was older than 55 years, she was designated postmenopausal (N = 139). For women in the intermediate age group (43–55 years old), FSH (follicular stimulating hormone) levels were measured and used to assign menopausal status primarily based upon the manufacturer's test guidelines (premenopausal cutoff: FSH <=15 mIU/ml, postmenopausal cutoff: FSH >=23 mIU/ml) (*20*). Of those in the intermediate age range and assigned by FSH values (N = 152), 75 were designated premenopausal, 60 were postmenopausal, and the others were in between the two cutoff values and were designated perimenopausal (N = 17). Due to the paucity of samples collected from perimenopausal women, they were excluded. The final data set included 492 samples collected from 412 women (293 premenopausal and 199 postmenopausal samples). Of the 80 subjects with two separate samples, 63 had samples that were both collected prior to menopause, 6 subjects had samples that were both collected after menopause, and 11 had one sample collected before and one after menopause.

All blood samples were obtained with informed consent, and the Human Investigation Committee of the Radiation Effects Research Foundation (RERF) approved the study protocol.

Sample Storage and Serum Assays

Sera were collected in the Hiroshima and Nagasaki laboratories between 1969 and 1992 and stored in vials at −80°C. Samples for this study were pulled from the freezers simultaneously and assayed for total E_2, bioavailable E_2, testosterone, progesterone, prolactin, IGF-1, IGFBP-3, ferritin, and total protein and protein fractions (albumin and globulin). All assays were performed blinded to age, city of collection and radiation exposure but were not performed in duplicate due to the limited serum amounts available. Commercial laboratories with internal quality assurance systems performed all assays. Supplementary Table 1 (http:dx.doi.org/10.1667/RR2631.1.S1) lists the assays and their precision as reported by the kits' manufacturers.

Serum levels of IGF-1, IGFBP-3, FSH, prolactin, testosterone, progesterone and ferritin were measured at a single laboratory (SRL Laboratory, Hachioji, Japan). Total protein concentration and protein fractions were measured by SRL using the Biuret method and cellulose acetate membrane electrophoresis, respectively. Serum levels of total E_2 and percentage bioavailable E_2 were measured at a single laboratory (Mitsubishi Kagaku Bio-clinical Laboratories, Tokyo, Japan). Percentage bioavailable E_2 (the fraction of serum E_2 that is free or loosely bound to albumin) was determined by ammonium sulfate precipitation of SHBG-bound E_2 (*21*). Total E_2 was multiplied by this percentage to obtain the concentration of bioavailable E_2. Serum ferritin was measured by the conventional chemiluminescence enzyme immunoassay (CLEIA). When the aliquots of samples were transported to outside laboratories for testing, they were packed in appropriate protective shipping boxes with sufficient amounts of dry ice and checked at the time of receipt by the measuring laboratories.

Methods of Analysis

Due to the skewed distributions of the markers, analyses were performed using log-transformed values for all of the markers except IGF1 and IGFBP-3, which did not require transformation. Effects of radiation exposure were estimated with adjustment only for other factors that were significantly related to marker level for statistical efficiency. Explanatory factors considered were: age at time of sample collection, year of birth, menopausal status (pre or post), total protein, body mass index [weight (kg)/height (m^2)] and its square, history of exogenous hormone use (yes or no), age at time of radiation exposure (including dichotomy at 15 years as a surrogate for pre- or postmenarche at time of exposure), number of full-term pregnancies, age at first full-term delivery, and radiation dose. Decisions for inclusion of factors other than radiation dose were based on a backward selection process where the least significant explanatory factor was removed until all factors were significant at a level of $P \leq 0.05$. The variable selection process was conducted separately for each marker. Analyses were performed using a regression method for correlated (repeated) measurements (generalized estimating equations; GEE) (*22*). P values and 95% confidence intervals were based on the Wald statistic.

TABLE 1
Characteristics of Study Cohort and Collected Samples by Menopausal Status

Variable	Premenopausal samples (N = 293)	Postmenopausal samples (N = 199)	P value[a]
City (Hiroshima/Nagasaki)[b]	187/106	145/54	0.036
	Mean (range)	Mean (range)	
Age ATB (years)	13.4 (1.0–24.0)	28.2 (12.0–49.0)	<0.001
Age at collection (years)	40.3 (26.3–51.9)	57.7 (43.0–78.9)	<0.001
Radiation dose (weighted gray)	0.54 (0.0–3.2)	0.49 (0.0–2.8)	0.472
BMI (kg/m^2)	22.4 (15.6–32.4)	22.8 (14.6–39.3)	0.267
Number of full-term pregnancies	2.7 (0–11)	3.6 (0–11)	<0.001
Year of sample collection	1971.9 (1969–1991)	1975.4 (1970–1992)	<0.001
IGF-1 (ng/ml)	116.0 (0.0–320.0)	94.6 (62–130)	<0.001
IGFBP-3 (μg/ml)	2.53 (0.4–4.3)	2.37 (2.1–2.8)	0.002
	Median (interquartile range[c])	Median (interquartile range[c])	
Total E_2 (pg/ml)	86.65 (59.2–116.0)	18.50 (13.1–25.2)	<0.001
Bioavailable E_2 (pg/ml)	39.48 (27.3–53.7)	9.19 (5.8–13.2)	<0.001
Testosterone (ng/dl)	15.7 (10.4–23.3)	10.5 (6.7–18.3)	<0.001
Progesterone (ng/ml)	1.60 (0.40–10.0)	0.25 (0.19–0.30)	<0.001
Prolactin (ng/ml)	6.20 (4.0–9.2)	3.60 (2.4–5.1)	<0.001
Ferritin (ng/ml)	21.50 (7.5–41.0)	50.00 (29–94)	<0.001

Notes. The upper section is the count of samples by city. The middle section shows the averages and ranges of non-transformed variables. The bottom section shows the median and interquartile ranges of natural log-transformed variables.

[a] Counts tested with χ^2 test for independence, means tested with t test for equality, medians tested with the Wilcoxon rank-sum test for independent samples.

[b] 412 subjects (Hiroshima, N = 267/Nagasaki, N = 145). 80 subjects had multiple samples (63 subjects with two premenopausal samples, 6 subjects with two postmenopausal samples, 11 subjects with one premenopausal sample and one postmenopausal sample).

[c] 25th percentile to the 75th percentile.

Radiation effects were assessed using linear dose–response functions. Dose responses were estimated with and without regard to effect modification by menopausal status at the time of blood collection and ionizing radiation exposure before or after age 15. For markers that were transformed prior to analyses, the radiation effects were reported on the untransformed scale by exponentiating the regression coefficient obtained using the log-transformed data and represent the association between 1 Gy radiation dose and the percentage change in geometric mean of the marker level. IGF1 and IGFBP-3, which were not transformed, were also reported on a relative scale by dividing the dose coefficient by the regression constant. To test the strength of the observed radiation effects, we identified and removed the most influential observations using the size-adjusted criterion 2/sqrt(n) for the t-statistic-like standardized deletion diagnostic DFBETAS of Belsley *et al.* (*23*). To alleviate concerns about misclassification of menopausal status at the time of sample collection due to possible nonspecificity of the FSH results, we conducted a sub-analysis after restricting samples to those collected from women at ages less than 43 or greater than 55 (135 samples omitted) and compared results to the full analyses.

Statistical comparisons between samples collected pre- and postmenopause were performed using χ^2 tests (for counts), t tests for equality (for means) and Wilcoxon rank-sum tests for independent samples (for medians). Interactions of radiation effects by menopausal status or exposure before or after age 15 were tested using the likelihood ratio. To compare fits of statistically significant non-nested interaction models, the quasi-likelihood/independence criterion (QIC) was used (*24*). All results were obtained using Stata (*25*).

RESULTS

Table 1 shows the demographics of the study cohort and marker values for samples separated by menopausal status at the time of collection. The distribution of the radiation dose is broader than what would be expected from a random sampling of all cancer-free women since they were counter-matched (low, medium, high) against the dose status of the case to ensure a broad representation of doses. The average year of sample collection is somewhat later for postmenopausal samples because the AHS study is a fixed cohort; more women were postmenopausal in later calendar years.

Table 2 shows the agreement of assays for the 63 pairs of samples collected from women who were premenopausal at each collection. Comparisons of multiple samples collected from the same women while postmenopausal were not reported (N = 6 pairs). The earlier sample was collected at average age 39.7 years and the average interval between sample collections was 2.8 years. Correlation coefficients ranged from 0.11 for progesterone to 0.75 for ferritin. A paired t test comparing the difference of the paired values with zero was not significant for any marker except for serum prolactin, where the earlier value proved to be significantly higher than the second value.

The first column of Table 3 shows the associations of radiation with marker levels with no allowance for effect modification but with adjustment for other significant factors. No significant radiation associations were observed in any of the markers when ignoring menopausal status. Columns two through five in Table 3 show the radiation associations separately by menopausal status at the time of sample collection or by age

TABLE 2
Comparison of Assay Values from Women Donating Multiple Samples

Assayed biomarker	*N*	Sample 1 average value (SD)	Sample 2 average value (SD)	Correlation	Sample 1 − Sample 2 average value (SD)	*P* value
Log total E_2 (pg/ml)	63	4.47 (1.02)	4.34 (0.54)	0.14	0.13 (1.10)	0.10
Log bioavailable E_2 (pg/ml)	63	3.65 (0.94)	3.64 (0.54)	0.16	0.014 (1.03)	0.42
Log testosterone (ng/dl)	57	2.74 (0.59)	2.74 (0.59)	0.52	0.0066 (0.54)	0.55
Log progesterone (ng/ml)	54	0.49 (1.71)	0.53 (1.64)	0.11	−0.042 (2.3)	0.54
Log prolactin (ng/ml)	57	1.86 (0.85)	1.47 (0.61)	0.28	0.39 (0.91)	0.001
Log ferritin (ng/ml)	56	3.12 (1.30)	3.11 (1.35)	0.75	0.0082 (0.83)	0.93
IGF-1 (ng/ml)	57	129.0 (69.7)	149 (67.9)	0.16	−20.3 (88.1)	0.19
IGFBP-3 (μg/ml)	57	2.51 (0.55)	2.54 (0.43)	0.36	−0.029 (0.60)	0.96

Notes. Samples are confined to multiple premenopausal samples (there were only six persons who donated multiple postmenopausal samples). The average age at the time of Sample 1 collection was 37.9 years and the average year of collection was 1970.9. The average age at the time of collection for the second sample was 40.8 years and the average year of collection was 1973.7. Values in parentheses (SD) after averages are standard deviations. The *P* value in the last column is a paired *t* test (H_o: Sample 1 − Sample 2 = 0).

at time of bombing (≤15 or >15 years; ATB15). Because menopausal status at blood donation was highly correlated with ATB15 in this study sample (particularly for a woman's first/only serum sample), the latter two columns largely mirror the results displayed in the former two. Total and bioavailable E_2, testosterone and IGF-1 demonstrated statistically significant associations with radiation dose in one or both periods.

Total E_2 (Fig. 1) decreased with radiation dose in the premenopausal period (relative change 0.89 at 1 Gy; 95% CI: 0.80, 0.99; $P = 0.027$), or in other words, the level of total E_2 changed as $k*0.89^{dose}$, where k is the level of total E_2 when the dose was zero (results from other log-transformed variables are interpreted in the same way). The level of total E_2 increased with dose in the postmenopausal period (relative change 1.17 at 1 Gy; 95% CI: 1.01, 1.36; $P = 0.037$). Effect modification by menopausal status was highly significant ($P = 0.003$) and remained significant after removing the most influential values ($P = 0.038$). The association of total E_2 with radiation dose was similar when categorizing subjects based on ATB15 (rather than menopausal status at the time of collection); relative change for a 1-Gy dose at age less than 15 years was 0.86 (95% CI: 0.76, 0.96; $P = 0.010$) and relative change for exposure after age 15 was 1.12 (95% CI: 0.99, 1.26; $P = 0.063$). Models used to estimate the radiation effects on total E_2 included menopausal status, age at sample collection, total protein, BMI and a BMI*postmenopause interaction. The QIC values for the two models were very similar, but the value for the ATB15 interaction model was slightly lower (i.e. better fit) than for the model with interaction by menopausal status.

Bioavailable E_2 (Fig. 2) showed a significant decrease with radiation dose in the premenopausal period, with a relative change of 0.88 at 1 Gy (95% CI: 0.80, 0.98; $P = 0.022$) and a significant increase with radiation dose in the postmenopausal period with a relative change of 1.21 at 1 Gy (95% CI: 1.04, 1.40; $P = 0.011$). Effect modification by menopausal status was highly significant ($P < 0.001$) and remained so after exclusion of influential observations ($P = 0.003$). As with total E_2, bioavailable E_2 also demonstrated similar radiation effects according to whether exposure was before or after age 15 (0.87 at 1 Gy; 95% CI: 0.77, 0.98; $P = 0.019$ and a relative increase of 1.13 at 1 Gy; 95% CI: 1.00, 1.27; $P = 0.045$, respectively). The model used to estimate the radiation effects on bioavailable E_2 included menopause status, age at sample collection and total protein. Again the QIC value was slightly lower for the model with ATB15 interaction.

Testosterone (Fig. 3) exhibited an increase with radiation dose in the postmenopausal period (relative change 1.30 at 1 Gy; 95% CI: 1.13, 1.49; $P < 0.001$) and a marginally significant decrease with radiation dose in the premenopausal period (0.90 at 1 Gy; 95% CI: 0.81, 1.00; $P = 0.049$). Estimates of effect modification by menopausal status were highly significant when estimates were derived using all observations ($P < 0.001$) and after excluding outliers ($P = 0.003$), whereas no effect modification was evident with ATB15. The testosterone model included menopause status, age at sample collection, total protein and a total protein*postmenopause interaction, and BMI.

IGF-1 (Fig. 4) displayed a significant increase with radiation dose in the premenopausal period (relative change 1.11 per Gy; 95% CI: 1.02, 1.18; $P = 0.024$). Since the values from this assay were not log-transformed, the results are interpreted as the percentage change in marker levels per gray. No significant change with dose was observed in the postmenopausal period (relative change 0.91 per Gy; 95% CI: 0.75, 1.04; $P = 0.18$). Similar effects were seen when categorizing the women by age at exposure. Effect modification by menopausal status was significant ($P = 0.014$) and remained so after removing the most influential observations ($P = 0.017$). Comparing QIC values indicated that the model with menopausal interaction model was preferable to the one with ATB15 interaction. Estimates of the radiation effects were adjusted for age at sample collection, year of birth, total protein*premenopause interaction, and number of full-term pregnancies.

TABLE 3
Relative Radiation Associations with Adjusted Mean Marker Values and Effect Modification By Menopausal Status and Age at Radiation Dose

Marker	Relative radiation association at 1 Gy no effect modification (95% confidence intervals), *P* value	Relative radiation association at 1 Gy Separately by effect-modifier category[a] (95% confidence intervals), *P* value			
		Menopause status at time of sample collection		Age at time of the bomb	
		Pre (N = 293)	Post (N = 199)	≤15 (N = 190)	>15 (N = 302)
Total E_2[b,d]	0.97	0.89	1.17	0.86	1.12
	(0.89, 1.06)	(0.80, 0.99)	(1.01, 1.36)	(0.76, 0.96)	(0.99, 1.26)
	P = 0.52	**P = 0.027**	**P = 0.037**	**P = 0.010**	P = 0.063
		Interaction **P = 0.003**		Interaction **P = 0.002***	
Bioavailable E_2[b,e]	0.98	0.88	1.21	0.87	1.13
	(0.93, 1.06)	(0.80, 0.98)	(1.04, 1.40)	(0.77, 0.98)	(1.00, 1.27)
	P = 0.84	**P = 0.022**	**P = 0.011**	**P = 0.019**	**P = 0.045**
		Interaction **P <0.001**		Interaction **P = 0.002***	
Testosterone[b,f]	1.02	0.90	1.30	0.97	1.06
	(0.93, 1.12)	(0.81, 1.00)	(1.13, 1.49)	(0.84, 1.10)	(0.93, 1.20)
	P = 0.70	**P = 0.049**	**P < 0.001**	P = 0.617	P = 0.387
		Interaction **P < 0.001**		Interaction P = 0.337	
Progesterone[b,g]	1.08	1.08	1.10	1.00	1.21
	(0.90, 1.30)	(0.86, 1.35)	(0.81, 1.50)	(0.77, 1.29)	(0.93, 1.58)
	P = 0.39	P = 0.52	P = 0.54	P = 0.992	P = 0.16
		Interaction P = 0.905		Interaction P = 0.313	
Prolactin[b,h]	1.01	0.97	1.07	0.94	1.08
	(0.91, 1.11)	(0.86, 1.09)	(0.91, 1.26)	(0.82, 1.08)	(0.95, 1.24)
	P = 0.905	P = 0.641	P = 0.384	P = 0.413	P = 0.230
		Interaction P = 0.313		Interaction P = 0.161	
IGF-1[c,i]	1.04	1.11	0.91	1.11	0.98
	(0.96, 1.10)	(1.02, 1.18)	(0.75, 1.04)	(0.99, 1.20)	(0.85, 1.07)
	P = 0.29	**P = 0.024**	P = 0.18	P = 0.061	P = 0.850
		Interaction **P = 0.014***		Interaction **P = 0.091**	
IGFBP-3[c,j]	1	1.01	0.98	1.00	0.93
	(0.97, 1.03)	(0.97, 1.05)	(0.92, 1.05)	(0.97, 1.04)	(0.97, 1.03)
	P = 0.89	P = 0.48	P = 0.44	P = 0.81	P = 0.82
		Interaction P = 0.28		Interaction P = 0.98	
Ferritin[b,k]	0.97	0.98	0.96	0.87	1.07
	(0.83, 1.13)	(0.81, 1.18)	(0.73, 1.27)	(0.70, 1.09)	(0.86, 1.32)
	P = 0.72	P = 0.81	P = 0.78	P = 0.22	P = 0.55
		Interaction P = 0.92		Interaction P = 0.19	

Notes. Numbers in parentheses are 95% confidence intervals. The first column shows the radiation associations without adjustment for menopause status at the time of sample collection or age at the time of the exposure from the atomic bombings. The right two sets of columns show the radiation associations by menopause status (columns 2, 3) and age less than or greater than 15 at the time of the bombing (columns 4, 5). The "Interaction P" values test whether the results differ significantly by menopausal status or age at the time of the bombing. Note that there were no detected effects when effect modification was ignored. The models were developed using a backwards elimination process for statistical efficiency as described in the text. Covariates for each model are listed in the footnotes. All effect modification models included the main effect variable regardless of whether it was selected in the elimination process. *QIC value indicates that this interaction model was better than the alternative interaction model. This score was compared only between the two interaction models and only when both models were significant.

[a] Effects of radiation are displayed separately for each of two categories of either menopausal status at time of serum collection (pre- or postmenopause) or age at time of exposure (up to age 15 or after age 15). The main effect was always included when testing the interaction.

[b] Log-transformed variable (relative change is calculated using X^{dose}, where X is the reported coefficient).

[c] Non-transformed variable (relative change is calculated using X * dose, where X is the reported coefficient).

[d] Adjusted for age and menopause status at sample collection, total protein, BMI and BMI*postmenopause interaction.

[e] Adjusted for age and menopause status at sample collection, total protein.

[f] Adjusted for age and menopause status at sample collection, total protein, total protein*postmenopause interaction, BMI.

[g] Adjusted for menopause status at sample collection, total protein.

[h] Adjusted for age and menopause status at sample collection.

[i] Adjusted for age at sample collection, year of birth, total protein*premenopause interaction, number of full-term pregnancies.

[j] Adjusted for year of birth, total protein*premenopause interaction, BMI, BMI^2.

[k] Adjusted for age and menopausal status at sample collection, BMI, number of full-term pregnancies.

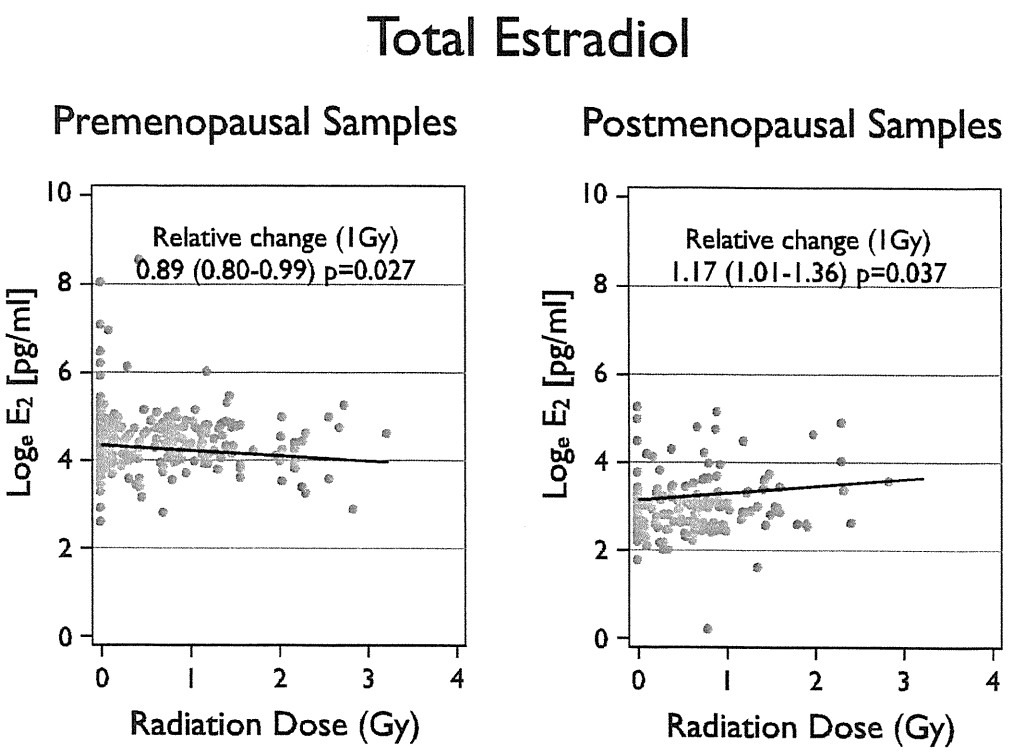

FIG. 1. Log total estradiol (E_2) by menopausal status and radiation dose. The relative change is the percentage change at a dose of 1 Gy. The regression lines and *P* values are based on the final models obtained for the markers (Table 3). The slopes of the two regression lines by menopausal status are significantly different ($P = 0.003$).

The other markers (IGFBP-3, progesterone, prolactin and ferritin) demonstrated no associations with radiation dose, either with or without effect modification. No effect modification of the radiation effects was observed in relation to the sample storage period, time since exposure, or the number of full-term pregnancies, although E_2 levels did increase at a marginally significant level for each additional full-term pregnancy (results not shown). Model fits generally improved when including the number of full-term pregnancies (as either an effect modifier or a main effect), but the estimated coefficients for the number of pregnancies were never statistically significant and therefore the results were not reported. No improvements in model fit were detected by the addition of a quadratic dose term. Point estimates were generally unchanged by the removal of samples retrieved when women were aged 43 to 55.

DISCUSSION

The present study was designed to investigate the associations of ionizing radiation exposure with sex and growth hormones in cancer-free A-bomb survivors using stored sera. Increasing levels of ionizing radiation exposure led to disparate changes by menopausal status in a number of serum markers. Levels of E_2 and bioavailable E_2 increased in postmenopausal samples while they decreased in premenopausal samples. Caution must be used when interpreting the results in premenopausal samples, especially E_2 levels, which are highly variable in premenopausal women due to the menstrual cycle. Table 2 illustrates the high variability of serum marker levels among premenopausal women. Controlling for the day of the menstrual cycle was not possible, because the clinical examination protocol did not attempt to record these values. It should be noted, however, that the point estimates for the radiation findings were largely unchanged after separately removing the most influential measurements (e.g., those associated with the E_2 peak at ovulation) and excluding those in the perimenopausal age range 43–55. Also, it is unlikely that there is any association with the timing of blood sample collection and radiation dose, eliminating most concerns of confounding. Nevertheless, chance findings for the premenopausal hormone associations cannot be completely ruled out.

The magnitude of change in total E_2 levels was about 10% at 1 Gy of radiation (negative in premenopausal women and positive in postmenopausal women). It is not clear that either of these are clinically significant changes, particularly among premenopausal women where there is so much variation. However, if E_2 levels were assigned to quartiles in samples taken from postmenopausal women, a 10% change in any particular result would generally be sufficient to increase its quartile assignment by one

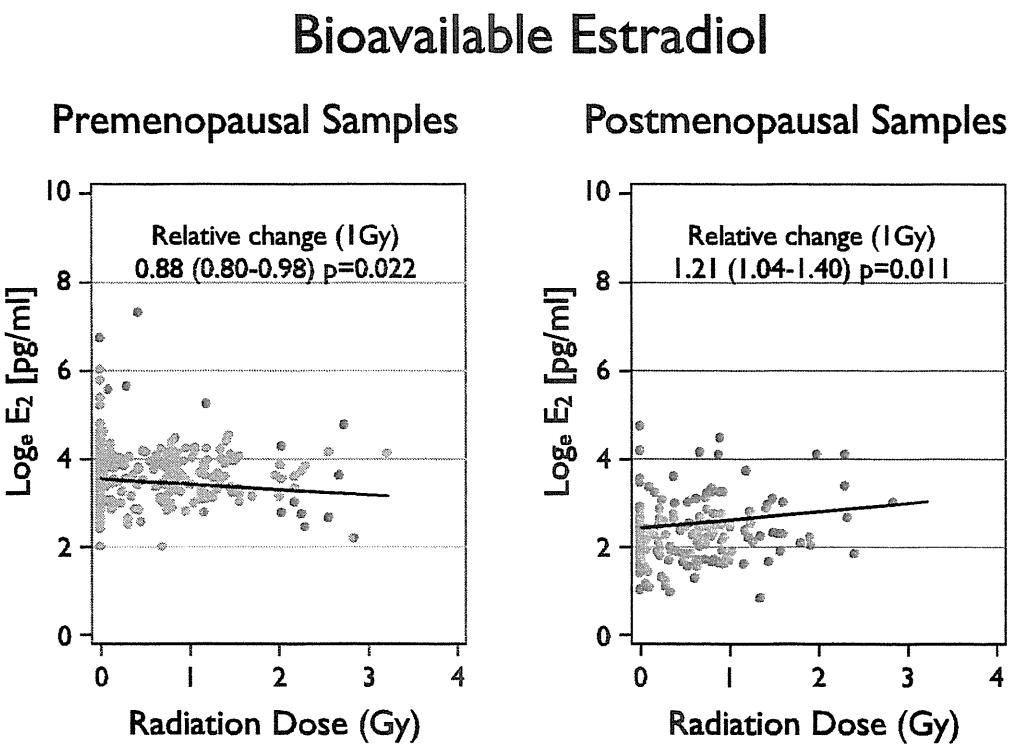

FIG. 2. Log bioavailable estradiol (E_2) concentration by menopausal status and radiation dose. The relative change is the percentage change at a dose of 1 Gy. The regression lines and *P* values are based on the final models obtained for the markers (Table 3). The slopes of the two regression lines by menopausal status are significantly different ($P < 0.001$).

category. Interpolating the results from Fig. 1 of the meta-analysis performed by Key *et al.* (*7*), this increase in total E_2 would roughly correspond to a 25% increase in breast cancer risk.

The significance of IGF-1 and IGFBP-3 levels in pre- or postmenopausal breast cancer has been under debate. The most recent evidence indicates that high levels of IGF-1 confer an increased risk of breast cancer (*10*). In our study, radiation exposure appeared to increase the level of IGF-1 in premenopausal women but had no effect on levels of IGF-1 in postmenopausal women. Again, however, large variations were observed in the premenopausal IGF-1 levels. IGFBP-3 was not associated with radiation exposure.

If the results are correct, questions arise regarding the radiation-related biological pathways that may affect sex hormone levels, particularly the most potent hormone E_2. In premenopausal women, E_2 is produced primarily by the ovaries whereas after ovarian involution, estrogen is primarily produced in adipose tissue by converting androgen to estrogen via aromatase. A number of speculative mechanisms for an association between radiation and sex steroid alterations can be suggested, including damage to primordial ovarian follicles leading to decreased ovarian aromatase and depressed E_2 production as observed in the samples taken from women who were exposed at less than 15 years of age (*26, 27*). Ataya *et al.* reported similar findings with decreased ovarian size and long-term decreased serum E_2 levels in rhesus monkeys with ovarian exposure to ionizing radiation (*28*). Larsen *et al.* reported decreased ovarian volume in spontaneously ovulating women who had received chemotherapy and radiotherapy for cancers diagnosed at mean age 5.4 years; however, E_2 levels were reported to be higher in those receiving (any type of) therapy compared to a control group of similar age (*29*).

For the results seen among older birth cohorts (i.e. postmenopausal samples), radiation-induced upregulation of inflammatory cytokines, specifically TNFα, can lead to increased estrogen biosynthesis (*30–33*); radiation can also alter lipid metabolism (*34–36*), possibly leading to hyperandrogenism through hypothalamus-pituitary-adrenal axis dysregulation (*37*). Either of these latter mechanisms would be consistent with the observed increased E_2 and testosterone levels among the postmenopausal women.

No effect modification by the number of full-term pregnancies was evident in the radiation effects on any of the markers. The number of women reporting any history of exogenous hormone intake was less than 10%, and that variable was not a significant risk factor in any of the tested models. Therefore, we do not believe that hormone treatment had a meaningful impact on our

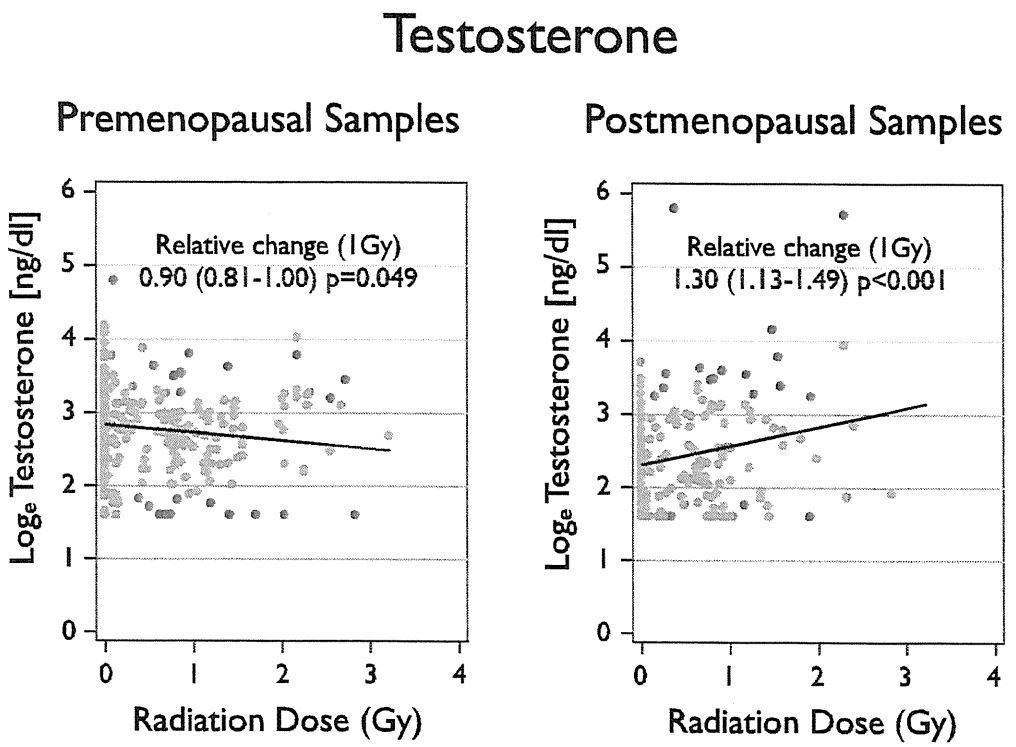

FIG. 3. Log testosterone by menopausal status and radiation dose. The relative change is the percentage change at a dose of 1 Gy. The regression lines and *P* values are based on the final models obtained for the markers (Table 3). The slopes of the two regression lines by menopausal status are significantly different ($P < 0.001$).

findings. Interaction models categorizing exposures before or after age 15 more often had a better fit than models categorized by menopausal status at the time of serum collection. However, this may be due to misclassification of menopausal status as opposed to an important biological effect involving menarche status at the time of radiation exposure. McDougall *et al.* found no association of breast cancer risk and menarche status at the time of radiation exposure but did not consider serum marker levels (*38*).

Associations of radiation and markers modified by menopausal status were tested in the results of eight bioassays (the two parallel analyses of modification by either menopause status or ATB15 are effectively the same), which may raise concerns of finding associations due to multiple testing. Using the conservative Bonferroni correction for multiple testing ($\alpha = 0.05/8 = 0.00625$), all of the tests for interaction remain significant with the exception of IGF-1 ($P = 0.014$).

The study boasts a number of strengths, including well-characterized radiation doses to a representative population of women, and data collected prospectively from cancer-free women as part of a long-term follow-up regimen, including medical history data on hormone-related conditions. However, there are also several weaknesses. The day of blood collection in relation to the menstrual cycle was not available, which is problematic for premenopausal estradiol measurements in particular. The use of FSH to assign menopausal status has been shown to be not fully specific (*39*). It is also likely that misclassification occurred when assigning menarche status by age. Due to the limited number of samples, duplicate assays for quality control were not attempted. A limited number of women did have multiple samples collected while premenopausal, for which the correlation between marker assays was generally poor, probably due to different times in the menstrual cycle. Despite these limitations, no major changes in the interactions between the measured radiation associations and menopausal status were detected after separately removing the most influential observations and those observations drawn from women in the perimenopausal age range, which helps confirm the robustness of the associations.

Conclusions

Previous studies have proven the potency of ionizing radiation as a carcinogen via direct damage effects to DNA while separate lines of research have established serum levels of E_2, testosterone and IGF1 as risk factors for breast cancer. The results of this study suggest that ionizing radiation may lead to changes in serum levels of cancer-related hormones and proteins in cancer-free women and that these changes are dependent upon

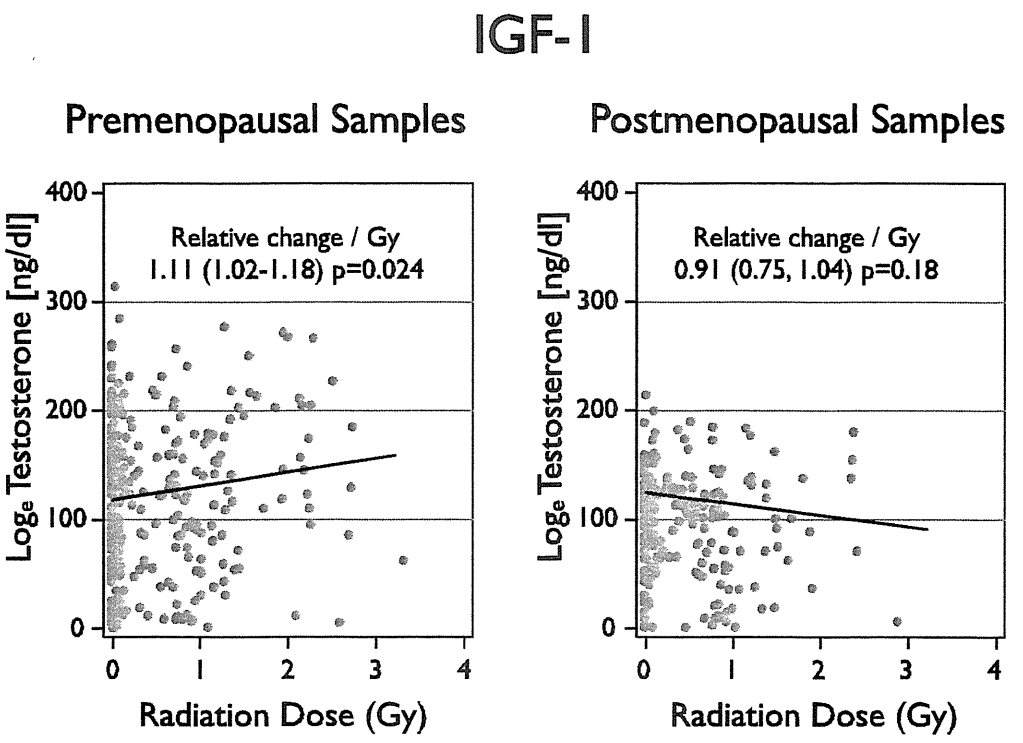

FIG. 4. IGF-1 by menopausal status and radiation dose. The relative change is the percentage change at a dose of 1 Gy. The regression lines and *P* values are based on the final models obtained for the markers (Table 3). The slopes of the two regression lines by menopausal status are significantly different ($P = 0.014$).

either the menopausal status at the time of collection or the menarche status at the time of exposure. Several mechanisms for these changes are suggested, but they are all speculative. Researchers of cancer etiology after whole-body ionizing radiation exposure should be aware of possible underlying changes in the levels of serum markers, which may confer independent carcinogenic risks.

ACKNOWLEDGMENTS AND FUNDING

We deeply thank the participating members of the AHS. The Radiation Effects Research Foundation (RERF), Hiroshima and Nagasaki, Japan is a private, non-profit foundation funded by the Japanese Ministry of Health, Labor and Welfare (MHLW) and the U.S. Department of Energy (DOE), the latter in part through the National Academy of Sciences. This publication was supported by RERF Research Protocol RP 06-02 and by US National Cancer Institute contract NO1-CP-31012 and the Japanese Ministry of Education, Culture, Sports, Science and Technology grants 14031227 and 15026220.

Received: March 27, 2011; accepted: May 24, 2011; published online: June 30, 2011

REFERENCES

1. Brenner DJ, Hall EJ. Computed tomography – an increasing source of radiation exposure. N Engl J Med 2007; 357:2277–84.
2. Preston DL, Mattsson A, Holmberg E, Shore R, Hildreth NG, Boice JD. Radiation effects on breast cancer risk: a pooled analysis of eight cohorts. Radiat Res 2002: 158:220–35.
3. Preston DL, Ron E, Tokuoka S, Funamoto S, Nishi N, Soda M, et al. Solid cancer incidence in atomic bomb survivors: 1958–1998. Radiat Res 2007; 168:1–64.
4. UNSCEAR. Sources and effects of ionizing radiation. United Nations Scientific Committee on the Effects of Atomic Radiation: UNSCEAR 2000 Report to the General Assembly, with scientific annexes; 2000.
5. Hankinson SE, Willett WC, Manson JE, Colditz GA, Hunter DJ, Spiegelman D, et al. Plasma sex steroid hormone levels and risk of breast cancer in postmenopausal women. J Natl Cancer Inst 1998; 90:1292–9.
6. Toniolo PG, Levitz M, Zeleniuch-Jacquotte A, Banerjee S, Koenig KL, Shore RE, et al. A prospective study of endogenous estrogens and breast cancer in postmenopausal women. J Natl Cancer Inst 1995; 87:190–7.
7. Endogenous Hormones and Breast Cancer Collaborative Group, Key T, Appleby PN, Reeves GK, Roddam AW. Endogenous sex hormones and breast cancer in postmenopausal women: reanalysis of nine prospective studies. J Natl Cancer Inst 2002; 94:606–16.
8. Henderson BE, Feigelson HS. Hormonal carcinogenesis. Carcinogenesis 2000; 21:427–33.
9. Russo J, Russo IH. Genotoxicity of steroidal estrogens. Trends Endocrinol Metab 2004; 15:211–4.
10. Endogenous Hormones and Breast Cancer Collaborative Group, Key T, Appleby PN, Reeves GK, Roddam AW. Insulin-like growth factor 1 (IGF1), IGF binding protein 3 (IGFBP3), and breast cancer risk: pooled individual data analysis of 17 prospective studies. Lancet Oncol 2010; 11:530–42.
11. Renehan AG, Zwahlen M, Minder C, O'Dwyer ST, Shalet SM, Egger M. Insulin-like growth factor (IGF)-I, IGF binding protein-3, and cancer risk: systematic review and meta-regression analysis. Lancet 2004; 363:1346–53.
12. Kaaks R, Berrino F, Key T, Rinaldi S, Dossus L, Biessy C, et al. Serum sex steroids in premenopausal women and breast cancer

risk within the European Prospective Investigation into Cancer and Nutrition (EPIC). J Natl Cancer Inst 2005; 97:755–65.

13. Tworoger SS, Eliassen AH, Sluss P, Hankinson SE. A prospective study of plasma prolactin concentrations and risk of premenopausal and postmenopausal breast cancer. J Clin Oncol 2007; 25:1482–8.
14. Russo J, Hu YF, Silva ID, Russo IH. Cancer risk related to mammary gland structure and development. Microsc Res Tech 2001; 52:204–23.
15. Yamada M, Wong FL, Fujiwara S, Akahoshi M, Suzuki G. Noncancer disease incidence in atomic bomb survivors, 1958–1998. Radiat Res 2004; 161:622–32.
16. (Young RW, Kerr GD, editors. Reassessment of the atomic bomb radiation dosimetry for Hiroshima and Nagasaki–Dosimetry System 2002. Hiroshima, Japan: Radiation Effects Research Foundation; 2005. 998 p.
17. Cologne JB, Sharp GB, Neriishi K, Verkasalo PK, Land C, Nakachi K. Improving the efficiency of nested case-control studies of interaction by selecting controls using counter matching on exposure. Int J Epidemiol 2004; 33:485–92.
18. Biesheuvel CJ, Vergouwe Y, Oudega R, Hoes AW, Grobbee DE, Moons KG. Advantages of the nested case-control design in diagnostic research. BMC Med Res Methodol 2008; 8:48.
19. Pierce DA, Stram DO, Vaeth M. Allowing for random errors in radiation dose estimates for the atomic bomb survivor data. Radiat Res 1990; 123:275–84.
20. Tokyo Special Reference Laboratories (SRL), Inc [Internet]. 卵胞刺激ホルモン (FSH) 基準値 [Follicle-stimulating hormone (FSH) reference levels]. [cited 2010 Jun 7]. Available from: http://www.srl.info/srlinfo/news/2003-14.htm. Japanese.
21. Pearce S, Dowsett M, Jeffcoate SL. Three methods compared for estimating the fraction of testosterone and estradiol not bound to sex-hormone-binding globulin. Clin Chem 1989; 35:632–5.
22. Liang KY, Zeger SL. Longitudinal data analysis using generalized linear models. Biometrika 1986; 73:13–22.
23. Belsley DA, Kuh E, Welsch RE. Regression diagnostics: identifying influential data and sources of collinearity. New York: Wiley; 1980.
24. Pan W. Akaike's information criterion in generalized estimating equations. Biometrics 2001; 57:120–5.
25. StataCorp. Stata Statistical Software: Release 11. College Station, TX: StataCorp LP; 2009.
26. Lee CJ, Yoon YD. Gamma-radiation-induced follicular degeneration in the prepubertal mouse ovary. Mutat Res 2005; 578: 247–55.
27. Lee YK, Chang HH, Kim WR, Kim JK, Yoon YD. Effects of gamma-radiation on ovarian follicles. Arhiv za higijenu rada i toksikologiju 1998; 49:147–53.
28. Ataya K, Pydyn E, Ramahi-Ataya A, Orton CG. Is radiation-induced ovarian failure in rhesus monkeys preventable by luteinizing hormone-releasing hormone agonists?: Preliminary observations. J Clin Endocrinol Metab 1995; 80:790–5.
29. Larsen EC, Müller J, Schmiegelow K, Rechnitzer C, Andersen AN. Reduced ovarian function in long-term survivors of radiation- and chemotherapy-treated childhood cancer. J Clin Endocrinol Metab 2003; 88:5307–14.
30. Frasor J, Weaver A, Pradhan M, Mehta K. Synergistic up-regulation of prostaglandin E synthase expression in breast cancer cells by 17β-estradiol and proinflammatory cytokines. Endocrinology 2008; 149:6272–9.
31. Salama S, Kamel M, Diaz-Arrastia C, Xu X, Veenstra TD, Salih S, et al. Effect of tumor necrosis factor on estrogen metabolism and endometrial cells: potential physiological and pathological relevance. J Clin Endocrinol Metab 2008; 94:28–93.
32. Hayashi T, Morishita Y, Kubo Y, Kusunoki Y, Hayashi I, Kasagi F, et al. Long-term effects of radiation dose on inflammatory markers in atomic bomb survivors. Am J Med 2005; 118:83–6.
33. Nakachi K, Hayashi T, Imai K, Kusunoki Y. Perspectives on cancer immuno-epidemiology. Cancer Sci 2004; 95:921–9.
34. Bezemer ID, Rinaldi S, Dossus L, Gils CH, Peeters PH, Noord PA, et al. C-peptide, IGF-I, sex-steroid hormones and adiposity: a cross-sectional study in healthy women within the European Prospective Investigation into Cancer and Nutrition (EPIC). Cancer Causes Control 2005; 16:561–72.
35. Akahoshi M, Amasaki Y, Soda M, Hida A, Imaizumi M, Nakashima E, et al. Effects of radiation on fatty liver and metabolic coronary risk factors among atomic bomb survivors in Nagasaki. Hypertens Res 2003; 26:965–70.
36. Wong FL, Yamada M, Sasaki H, Kodama K, Hosoda Y. Effects of radiation on the longitudinal trends of total serum cholesterol levels in the atomic bomb survivors. Radiat Res 1999; 151:736–46.
37. Pasquali R. Obesity and androgens: facts and perspectives. Fertil Steril 2006; 85:1319–40.
38. McDougall JA, Sakata R, Sugiyama H, Grant E, Davis S, Nishi N, et al. Timing of menarche and first birth in relation to risk of breast cancer in A-bomb survivors. Cancer Epidemiol Biomarkers Prev 2010; 19:1746–54.
39. Henrich JB, Hughes JP, Kaufman SC, Brody DJ, Curtin LR. Limitations of follicle-stimulating hormone in assessing menopause status: findings from the National Health and Nutrition Examination Survey (NHANES 1999–2000). Menopause 2006; 13:171–7.

Human Immunology 72 (2011) 821-826

Contents lists available at SciVerse ScienceDirect

journal homepage: www.elsevier.com/locate/humimm

Lymphocyte subset characterization associated with persistent hepatitis C virus infection and subsequent progression of liver fibrosis

Kengo Yoshida [a,*], Waka Ohishi [b], Eiji Nakashima [c], Saeko Fujiwara [b], Masazumi Akahoshi [d], Fumiyoshi Kasagi [e,f], Kazuaki Chayama [g], Masayuki Hakoda [h], Seishi Kyoizumi [a], Kei Nakachi [a], Tomonori Hayashi [a], Yoichiro Kusunoki [a,*]

[a] Department of Radiobiology/Molecular Epidemiology, Radiation Effects Research Foundation, Hiroshima, Japan
[b] Department of Clinical Studies, Radiation Effects Research Foundation, Hiroshima, Japan
[c] Department of Statistics, Radiation Effects Research Foundation, Hiroshima, Japan
[d] Department of Clinical Studies, Radiation Effects Research Foundation, Nagasaki, Japan
[e] Department of Epidemiology, Radiation Effects Research Foundation, Hiroshima, Japan
[f] Institute of Radiation Epidemiology, Radiation Effects Association, Tokyo, Japan
[g] Department of Medicine and Molecular Science, Division of Frontier Medical Science, Programs for Biomedical Research, Graduate School of Biomedical Sciences, Hiroshima University, Hiroshima, Japan
[h] Department of Nutritional Sciences, Faculty of Human Ecology, Yasuda Women's University, Hiroshima, Japan

ARTICLE INFO

Article history:
Received 23 March 2011
Accepted 20 May 2011
Available online 15 June 2011

Keywords:
Cohort study
Hepatitis C virus
Liver fibrosis
Lymphocyte subset

ABSTRACT

This study aims to deepen the understanding of lymphocyte phenotypes related to the course of hepatitis C virus (HCV) infection and progression of liver fibrosis in a cohort of atomic bomb survivors. The study subjects comprise 3 groups: 162 HCV persistently infected, 145 spontaneously cleared, and 3,511 uninfected individuals. We observed increased percentages of peripheral blood T_H1 and total CD8 T cells and decreased percentages of natural killer (NK) cells in the HCV persistence group compared with the other 2 groups after adjustment for age, gender, and radiation exposure dose. Subsequently, we determined that increased T_H1 cell percentages in the HCV persistence group were significantly associated with an accelerated time-course reduction in platelet counts—accelerated progression of liver fibrosis—whereas T_C1 and NK cell percentages were inversely associated with progression. This study suggests that T_H1 immunity is enhanced by persistent HCV infection and that percentages of peripheral T_H1, T_C1, and NK cells may help predict progression of liver fibrosis.

1. Introduction

Hepatitis C virus (HCV) infects some 120 to 170 million people worldwide, and persistent HCV infection is a major cause of liver diseases, including chronic hepatitis, cirrhosis, and hepatocellular carcinomas [1,2]. Both innate and adaptive arms of the host immune system are closely involved in persistent infection, liver injury, and virus clearance [3,4]. For instance, cytotoxic granule release and cytokine production of natural killer (NK) cells are inhibited by direct binding of HCV envelope protein E2 to CD81 on NK cells or stabilizing the human leukocyte antigen (HLA)-E expressions on hepatocytes in HCV-infected patients [5,6]. However, the comprehensive understanding of interactions between HCV and the immune system remains incomplete [3,4]. Moreover, aging, gender, and several environmental factors, such as alcohol drinking, smoking, and ionizing radiation, have been reported to influence host immune functions as well as HCV spontaneous clearance [7–9], which may increase the complexity of virus–host interactions. Therefore, a comprehensive characterization of host immunologic phenotypes in HCV infection is needed, especially with a cohort-based study design without conceivable selection bias [10]. Nevertheless, few studies along those lines have been carried out. One prospective cohort study (the Adult Health Study [AHS]) of atomic bomb survivors—a longevity cohort with biennial health examinations—has been conducted at the Radiation Effects Research Foundation (RERF) and provides clinicoepidemiological data related to HCV infection and immunologic status [11,12]. Within the cohort study, we conducted a cross-sectional analysis for peripheral blood lymphocyte subsets among HCV persistently infected, spontaneously cleared, and uninfected groups, aiming to delineate immunologic distinctions among these 3 groups. We also aimed to identify the lymphocyte subsets that can predict hepatitis progression in HCV-persistent individuals on the basis of a longitudinal analysis of time-course changes of platelet counts.

* Corresponding authors.
E-mail addresses: kyoshi@rerf.or.jp; ykusunok@rerf.or.jp (K. Yoshida; Y. Kusunoki).

0198-8859/11/$32.00 - see front matter © 2011 American Society for Histocompatibility and Immunogenetics. Published by Elsevier Inc. All rights reserved.
doi:10.1016/j.humimm.2011.05.029

2. Subjects and methods

2.1. Study population

The Atomic Bomb Casualty Commission, subsequently the RERF, established the AHS cohort in 1958. This cohort study enrolled a total of 23,000 atomic bomb survivors in Hiroshima and Nagasaki who biennially received health examinations in outpatient clinics [11]. Hepatitis screening (HBsAg, anti-HBc antibody (Ab), anti-HBs Ab, and anti-HCV Ab tests, as well as HCV RNA test if the anti-HCV Ab was positive) was conducted among 6,121 AHS participants in 1993–1995 [12]. Anti-HCV Ab negative subjects were categorized as the HCV-uninfected group in this study, whereas a "persistence" group was identified by anti-HCV Ab positive with detected HCV RNA, and a "spontaneous clearance" group was identified by anti-HCV Ab positive and undetectable HCV RNA. Subjects who were hepatitis B virus surface antigen positive were excluded from this study. From the 6,121 AHS subjects, lymphocyte subsets in the peripheral blood were then examined in 162 HCV persistence, 145 virus clearance, and 3,511 uninfected subjects in 2000–2002. Most subjects (n = 120, 74%) in the persistence group (n = 162, including those with cancer history) were confirmed by a second RNA test at least 2 years after the first RNA test performed in 1993–1995. Although the remaining 42 subjects in the group did not undergo the second RNA test, these subjects were confirmed to have developed type C chronic liver disease based on medical chart review (*e.g.*, treatment history, abdominal sonographic observation, changes in platelet counts, zinc sulfate turbidity, aspartate aminotransferase (AST), and alanine aminotransferase (ALT) between 1993–1995 and 2000–2002) by a hepatologist (one of the authors, WO). Subsequent treatment data of hepatitis C from attending physicians were also taken into account. No subjects in the persistence group underwent interferon (IFN) therapy in 2000–2002.

This study was approved by the RERF Human Investigation Committee, and all subjects gave written informed consent before each examination.

2.2. Assays in hepatitis screening and clinical examinations

In 1993–1995, anti-HCV Ab and hepatitis B virus surface antigen were examined using a second-generation passive hemagglutination kit and a reverse passive hemagglutination kit (Dynabott, Tokyo), as described previously [12]. Subjects were diagnosed as having Ab when agglutination was reported in a serum diluted 2^5. Qualitative and quantitative detection of HCV RNA was carried out using the Amplicor HCV ver. 2.0 and the Amplicor HCV monitor test ver. 1.0 and/or ver. 2.0 (Roche Diagnostics Systems, Tokyo, Japan).

Platelet count decreases with progression of liver fibrosis, and this marker has widely been used as a reliable diagnostic tool for liver fibrosis/cirrhosis in patients with chronic HCV infection [13–16]. Postulated mechanisms for such platelet reduction include decreased secretion of the hematopoietic growth factor thrombopoietin from the liver and increased destruction of platelets by antiplatelet antibodies [17,18]. Platelet count was routinely measured in the AHS health examination, and an automatic blood cell counter (Coulter MAXM, Beckman Coulter, Inc, Tokyo, Japan) was used in 2000–2002. AST, ALT, γ-glutamyltransferase (γ-GTP), and total cholesterol were also routinely measured, and an autoanalyzer (Hitachi 7180, Hitachi, Ltd., Tokyo, Japan) was used in 2000–2002.

2.3. Information on lifestyle/environmental factors and clinical data

Information on alcohol drinking and smoking was obtained from questionnaires at the time of the AHS health examination in 1993–1995 and 2000–2002, respectively. Body mass index (BMI) was measured at the AHS health examination in 2000–2002. Radiation dose was estimated by the DS02 dosimetry system [19], based on the weighted skin dose computed as the γ dose plus 10 times the neutron dose. No subjects were diagnosed with human immunodeficiency virus infection. No subjects underwent organ transplantation or immunosuppressive therapy. Clinical information was obtained at the AHS examination in 2000–2002 as well as medical chart review and classified according to the International Classification of Diseases code.

2.4. Lymphocyte subset analysis

Circulating T_H1 and T_H2 cells can be straightforwardly enumerated by flow cytometry, using cell surface markers for chemokine receptor, CXCR3, and prostaglandin D receptor, CRTH2, respectively [20,21]. CD8 T cells expressing CXCR3, known as T_C1, are also involved in viral control during HCV infection [22]. We thus focused on T_H1, T_H2, T_C1, and T_C2 cell subsets, as well as total CD4 T and CD8 T, NK, and B-cell subsets in relation to HCV infection status.

Analytical flow cytometry was conducted in a FACScan machine (BD Biosciences, San Jose, CA) as described previously [23]. Monoclonal antibodies as specific cell surface markers were purchased from BD Pharmingen (San Diego, CA), unless otherwise noted. CD4 or CD8 T cells were enumerated as PerCP-labeled CD3 positive and PE–CD4 or FITC–CD8 positive cells; CD16 or CD20 cells were enumerated as PerCP–CD3 negative and FITC–CD16 (Beckman Coulter, Brea, CA) or PE–CD20 positive cells. We used CXCR3 as a marker for T_H1 and T_C1 cells [20,22] and CRTH2 for T_H2 and T_C2 cells [21]. Namely, T_H1 and T_H2 cells were identified with PerCP–CD4, FITC–CXCR3 (R&D Systems, Minneapolis, MN), and biotinylated CRTH2 (kindly provided by Dr K. Nagata, BML, Kawagoe, Japan) plus PE-streptavidin; T_C1 and T_C2 cells were identified with PerCP–CD8, FITC–CXCR3, and biotinylated CRTH2 plus PE–streptavidin. In every measurement, approximately 20,000 cells were analyzed.

2.5. Statistical analysis

Two-sample Wilcoxon or Pearson χ^2 tests were performed to compare distributions of age, gender, city, radiation dose (Gy), smoking (packs/day), alcohol drinking (converted to grams of ethanol/day), BMI (kg/m^2), AST (IU/L), ALT (IU/L), γ-GTP (U/L), total cholesterol (mg/dL), and platelet count ($\times 10^4/\mu$L) among all combinations of the 3 groups.

Because aging and past radiation exposure likely influenced various immunologic markers [23], these events were also evaluated in this study. In each study group, the associations of lymphocyte subsets with age (at the time of examination), gender, radiation dose, and city were evaluated based on the multiple regression model [24]:

$$\log(\textit{subset percentages or ratios}) = \alpha + \beta_1 \times \textit{age} + \beta_2 \times \text{gender} + \beta_3 \times \text{dose} + \beta_4 \times \text{city} + \beta_5 \times \text{alcohol} + \beta_6 \times \text{smoking} + \beta_7 \times \text{BMI} + \beta_8 \times \text{autoimmune disease} + \beta_9 \times \text{allergic disease} + \beta_{10} + \textit{cancer} + \beta_{11} \times \text{other noncancer diseases},$$

where log is the logarithm at base 10, gender = 0 for male and 1 for female, and city = 1 for Hiroshima and 2 for Nagasaki. Smoking, alcohol drinking, BMI, autoimmune disease (1 if diagnosed, otherwise 0), allergic disease (1 or 0), cancer (1 or 0), and other noncancer diseases (*i.e.*, hypergammaglobulinemia and sarcoidosis, 1 or 0) were also used as additional explanatory variables.

We compared lymphocyte subset percentages or ratios among all combinations of the 3 groups in normal regression analysis with adjustment for age, gender, radiation dose, city, alcohol, smoking, BMI, autoimmune diseases, allergic diseases, and other noncancer diseases: In the regression analysis, an explanatory variable regarding a group (1 group = 0, another group = 1) was used.

Regression analysis was also performed to investigate whether any association existed between subset percentages or ratios and

Table 1
Characteristics of the study subjects

	Persistence (anti-HCV+/ HCV RNA+) (n = 162)	Clearance (anti-HCV+/ HCV RNA-) (n = 145)	Uninfected (anti-HCV-) (n = 3,511)	Persistence vs clearance (p)[a]	Persistence vs uninfected (p)[a]	Clearance vs uninfected (p)[a]
Age[b]	71.7 (60.8–83.0)	72.3 (64.8–88.0)	72.2 (58.4–87.2)	0.041	0.79	0.029
Gender[c]						
Male	57 (35.2)	48 (33.1)	1078 (30.7)	0.70	0.23	0.54
Female	105 (64.8)	97 (66.9)	2433 (69.3)			
City[c]						
Hiroshima	112 (69.1)	96 (66.2)	2034 (57.9)	0.58	0.005	0.048
Nagasaki	50 (30.9)	49 (33.8)	1477 (42.1)			
Radiation dose (Gy)[b]	0.147 (0–2.658)	0.071 (0–1.890)	0.096 (0–2.032)	0.26	0.47	0.39
Smoking (packs/day)[b]	0 (0–1.0)	0 (0–1.0)	0 (0–1.0)	0.80	0.087	0.18
Alcohol drinking (grams/day)[b]	0 (0–85.0)[d]	0 (0–103.0)[d]	0 (0–69.8)[d]	0.35	0.57	0.062
BMI (kg/m^2)[b]	22.4 (16.7–28.5)	22.6 (17.3–29.6)	22.7 (17.6–28.7)	0.46	0.084	0.58
AST (IU/L)[b]	21 (15–51)	21 (14–35)	22 (15–43)	0.15	0.85	0.081
ALT (IU/L)[b]	17 (9–46)	18 (9–42)	17 (9–44)	0.87	0.99	0.84
γ-GTP (U/L)[b]	28.5 (12.5–131.5)	25 (12–127)	24 (11–111)	0.10	<0.001	0.29
Total cholesterol (mg/dL)[b]	168.5 (117–234)	206 (142–264)	208 (154–266)	<0.001	<0.001	0.41
Platelet count (×10^4/μL)[b]	17.3 (7.2–28.2)	22.0 (14.3–30.8)	22.9 (14.5–33.7)	<0.001	<0.001	0.031

[a]Two-sample Wilcoxon rank-sum test or Pearson's χ^2 test for gender and city.
[b]Median (5–95% percentiles).
[c]Number (%).
[d]The percentages of never-drinkers were 59.3, 53.8, and 60.6 in the 3 groups, respectively.

time-course changes in platelet counts through the period from 2000 through 2006. Changes in platelet counts were calculated by the following method:

(platelet counts at the last examination

– platelet counts at the first examination)/follow-up years

In a regression analysis, a forward stepwise procedure was used for 8 immunologic variables, %CD4, T_H1, T_H2, CD8, T_C1, T_C2, CD16, and CD20. Four variables (%T_H1, T_C1, CD16, and CD20) were consequently selected (significance level to select, $p < 0.2$) to construct a statistical model. All analyses were conducted using Stata software (Stata/SE 9.2 for Windows, StataCorp LP, College Station, TX).

3. Results

3.1. Basic characteristics of study subjects

Table 1 compares characteristics of study subjects in the HCV persistence, clearance, and uninfected groups. The persistence group exhibited increased levels of blood γ-GTP and decreased levels of total cholesterol and platelet counts compared with the other 2 groups, indicating enhanced liver injury by persistent HCV infection. The proportion of Hiroshima subjects in the persistence or clearance group was higher than that in the uninfected group. This is in accordance with the previous study that indicated a higher anti-HCV Ab prevalence in Hiroshima atomic bomb survivors than in Nagasaki survivors [12]. There were no significant differences in radiation dose by HCV infection status.

This study primarily aimed to evaluate immunologic alterations associated with HCV infection that might be modulated by age, gender, or past radiation exposure. Therefore, the effects of those factors on lymphocyte subsets were first analyzed and are summarized in the supplemental tables. In the uninfected group, we observed the following: (i) age- and dose-dependent decreases in total CD4 T cell percentages, (ii) higher total CD4 T-cell percentages in females than in males, (iii) no significant effects of age, gender, or radiation dose on total CD8 T-cell percentages, (iv) increased CD16 (NK) cell percentages with increasing age and higher percentages in males than in females, (v) increased T_H1 and T_H2 cell percentages with increasing age and dose, and (vi) both T_H1/T_H2 and T_C1/T_C2 cell ratios negatively or positively associated with age and female gender, respectively, but not with radiation dose (Suppl. Table 1). The

Table 2
Characteristics of the study subjects with no cancer history

	Persistence (anti-HCV+/ HCV RNA+) (n = 102)	Clearance (anti-HCV+/ HCV RNA-) (n = 113)	Uninfected (anti-HCV-) (n = 2,813)	Persistence vs clearance (p)[a]	Persistence vs uninfected (p)[a]	Clearance vs uninfected (p)[a]
Age[b]	71.5 (61.3–82.7)	72.3 (62.4–90.8)	72.0 (58.1–87.3)	0.026	0.64	0.021
Gender[c]						
Male	36 (35.3)	38 (33.6)	832 (29.6)	0.80	0.22	0.36
Female	66 (64.7)	75 (66.4)	1981 (70.4)			
City[c]						
Hiroshima	70 (68.6)	77 (68.1)	1613 (57.3)	0.94	0.023	0.023
Nagasaki	32 (31.4)	36 (31.9)	1200 (42.7)			
Radiation dose (Gy)[b]	0.031 (0–1.862)	0.056 (0–1.890)	0.072 (0–1.878)	0.84	0.68	0.49
Smoking (packs/day)[b]	0 (0–1.0)	0 (0–1.0)	0 (0–1.0)	0.67	0.070	0.18
Alcohol drinking (grams/day)[b]	0 (0–90)[d]	0 (0–105.8)[d]	0 (0–69.8)[d]	0.067	0.76	0.014
BMI (kg/m^2)[b]	22.6 (16.7–28.5)	22.6 (17.3–29.6)	22.9 (17.7–28.8)	0.49	0.097	0.55
AST (IU/L)[b]	22 (15–50)	21 (13–37)	22 (15–42)	0.12	0.34	0.26
ALT (IU/L)[b]	18 (9–39)	17 (9–48)	17 (9–44)	0.57	0.69	0.69
γ-GTP (U/L)[b]	26 (12–100)	27 (12–127)	23 (11–106)	0.99	0.19	0.18
Total cholesterol (mg/dL)[b]	175 (124–243)	211 (136–272)	209 (157–266)	<0.001	<0.001	0.46
Platelet count (×10^4/μL)[b]	19.3 (10.3–32.0)	21.7 (14.2–30.8)	23.0 (14.8–33.7)	<0.001	<0.001	0.006

[a]Two-sample Wilcoxon rank-sum test, or Pearson's χ^2 test for gender and city.
[b]Median (5–95% percentiles).
[c]Number (%).
[d]The percentages of never-drinkers were 64.7, 50.4, and 61.1 in the 3 groups, respectively.

Table 3
Comparisons of peripheral lymphocyte subsets among subjects with no cancer history

	Persistence (n = 102)	Clearance (n = 113)	Uninfected (n = 2,813)	Persistence vs clearance (p)[a]	Persistence vs uninfected (p)[a]	Clearance vs uninfected (p)[a]
CD4 (%)[b]	40.8 (8.9)	42.2 (9.0)	43.0 (8.9)	0.32	0.007	0.46
T_H1 (%)[b]	35.2 (9.6)	27.1 (8.7)	26.0 (8.9)	<0.001	<0.001	0.23
T_H2 (%)[b]	1.55 (0.88)	1.74 (1.03)	1.79 (1.10)	0.54	0.11	0.65
T_H1/T_H2[b]	30.7 (20.6)	20.8 (12.8)	20.8 (23.0)	<0.001	<0.001	0.27
CD8 (%)[b]	23.4 (9.6)	20.9 (7.9)	19.0 (7.8)	0.20	<0.001	0.040
T_C1 (%)[b]	42.3 (14.7)	38.8 (15.2)	39.5 (14.6)	0.25	0.17	0.68
T_C2 (%)[b]	2.78 (3.72)	2.87 (4.03)	3.35 (5.09)	0.34	0.68	0.40
T_C1/T_C2[b]	42.8 (45.8)	50.9 (78.2)	51.1 (91.4)	0.66	0.38	0.51
CD4/CD8[b]	2.08 (1.02)	2.42 (1.35)	2.75 (1.57)	0.15	<0.001	0.054
CD16 (%)[b]	14.0 (9.4)	17.0 (8.8)	17.1 (9.4)	0.035	<0.001	0.82
CD20 (%)[b]	14.5 (7.6)	13.5 (5.3)	13.9 (6.1)	0.95	0.44	0.60

[a]Test of difference of logarithmic values between 2 groups using normal regression analysis with adjustment for age, gender, city, radiation dose, alcohol, smoking, BMI, autoimmune disease, allergic disease, and other noncancer diseases.
[b]Mean (SD).

persistence and clearance groups also demonstrated similar associations, although most associations were not statistically significant, probably because of the smaller numbers of subjects in these groups (Suppl. Tables 2 and 3). In addition to the 3 factors (age, gender, and radiation), other selected factors, such as city, alcohol, smoking, and BMI, also influenced various lymphocyte subsets (data not shown), and they were used as confounding variables in adjustments.

3.2. Comparison of lymphocyte subsets among the HCV persistence, clearance, and uninfected groups

The study subjects having cancer history numbered 60, 32, and 698 in the persistence, clearance, and uninfected groups, respectively. We then analyzed the lymphocyte subset alterations associated with HCV infection among subjects who have no history of cancer, presented in Table 2, to eliminate potential effects of cancer development and/or cancer therapy (Table 3). In addition, basic characteristics were not largely changed by excluding subjects with a history of cancer, but the radiation effects—specifically on T_H1 and T_H2 cells—were no longer seen among subjects with no cancer history (data not shown).

In the persistence group, T_H1 and total CD8 T cell percentages and T_H1/T_H2 ratios were significantly higher than those in the HCV-uninfected group, whereas total CD4 T and CD16 cell percentages were lower. Similar differences were also seen between the persistence and clearance groups. However, except for total CD8 T cell percentages, no significant differences were observed between the clearance and uninfected groups.

3.3. Relationship between lymphocyte subsets and progression of liver fibrosis in the HCV persistence group

Next, we analyzed the relationship between lymphocyte subsets and platelet counts that had been longitudinally examined at the biennial AHS examination during 2000–2006 in the HCV persistence group, excluding subjects with cancer history (Table 4). The average follow-up period was 4.7 years, and the average decrement of platelet counts per year was -0.75 ($\times 10^4/\mu L$). We determined that increased percentages of T_H1 cells were associated with accelerated time-course reduction in platelet counts—accelerated progression of liver fibrosis ($p = 0.027$)—whereas T_C1 and NK cell percentages were inversely associated with progression ($p = 0.027$ and 0.058, respectively).

4. Discussion

We investigated immunologic alterations associated with HCV infection in a longevity study cohort of atomic bomb survivors. First, the effects of age, gender, and radiation on total CD4 T, CD8 T, and NK cells were studied in the uninfected group (Suppl. Table 1) and observed to be in close agreement with our previous studies [9,23]. A new finding related to the uninfected group is that percentages of both T_H1 and T_H2 cells increased with increasing radiation dose and age. That result is consistent with our previous

Table 4
Regresson analysis of decrements (per year) in platelet counts among HCV persistence subjects with no cancer history (N = 96)

Explanatory variables	Unadjusted coefficient	p	Adjusted[a] coefficient	p	Adjusted[b] coefficient	p
Age (+10 years)	−0.26	0.33	–	–	–	–
Gender (female vs male)	0.43	0.21	–	–	–	–
Radiation dose (Gy)	0.28	0.26	–	–	–	–
City (Nagasaki vs Hiroshima)	0.00	0.99	–	–	–	–
Log CD4	−0.25	0.86	1.11	0.50	–	–
Log T_H1	−1.90	0.13	−2.38	0.086	−3.19	0.027
Log T_H2	−0.53	0.41	−0.34	0.65	–	–
Log T_H1/T_H2	0.03	0.97	−0.31	0.67	–	–
Log CD8	−1.72	0.060	−2.63	0.011	–	–
Log T_C1	1.66	0.068	2.05	0.041	2.36	0.027
Log T_C2	−0.30	0.37	0.23	0.57	–	–
Log T_C1/T_C2	0.51	0.12	0.10	0.81	–	–
Log CD4/CD8	1.04	0.16	2.03	0.015	–	–
Log CD16	0.73	0.21	1.13	0.062	1.18	0.058
Log CD20	1.10	0.11	1.04	0.15	1.03	0.17

[a]Regression model: decrements in platelet counts = $\alpha + \beta_1 \times log$(lymphocyte subset) + $\beta_2 \times$ age + $\beta_3 \times$ gender + $\beta_4 \times$ dose + $\beta_5 \times$ city + $\beta_6 \times$ alcohol + $\beta_7 \times$ smoking + $\beta_8 \times$ BMI + $\beta_9 \times$ autoimmune disease + $\beta_{10} \times$ allergic disease + $\beta_{11} \times$ other noncancer diseases.
[b]Forward stepwise procedure ($p < 0.2$) was used for 8 lymphocyte variables (CD4, T_H1, T_H2, CD8, T_C1, T_C2, CD16, and CD20). Four selected variables (T_H1, T_C1, CD16, and CD20) were used in the regression analysis with the 10 explanatory variables in footnote a.

findings in an expanded cohort of atomic bomb survivors, which demonstrated age- and radiation dose-dependent elevations of cytokine levels for both T_H1-related cytokines (IFN-γ and tumor necrosis factor-α) and a T_H2-related cytokine (interleukin [IL]-6) [25].

Second, we observed that persistent HCV infection was associated with increases in T_H1/T_H2 cell ratios and CD8 T cell percentages and a decrease in NK cell percentages (Table 3). Regarding cytokine responses to persistent HCV infection, past reports in diversified patient groups were rather inconsistent: enhanced T_H1 responses [26–29], T_H2 responses [30–32], or both types [33,34]. Although differing degrees of pathogenesis and/or inflammation among study patient groups may be in part responsible for this discrepancy [34,35], some potential methodological drawbacks in studies demonstrating T_H2 cytokine predominance were indicated [27]. The present study on lymphocyte subsets suggested enhanced T_H1 immunity in persistent HCV infection, supporting a view that enhanced T_H1 immunity alone is not sufficient to regulate the virus in many cases of HCV infection.

As observed in this study, both decreased and increased percentages of peripheral NK cells and total CD8 T cells, respectively, have been reported in HCV persistent individuals [36–39]. A reduction in NK cells is assumed to be linked to ongoing viremia that may induce continuous proliferation of CD8 T cells. A recent study on murine cytomegalovirus infection indicated that NK cells negatively regulated the number and activity of virus-specific CD8 T cells as well as CD4 T cells that played a critical role in limiting viral persistence; lack of NK cell activation resulted in increased numbers of CD8 T and CD4 T cells along with enhanced effector functions through antigen presentation by viral-infected antigen-presenting cells [40]. Such functional interplay among NK cells, antigen-presenting cells, and CD8 T cells may be common in virally infected hosts. It is also plausible that reduced NK cells of individuals may in part reflect their weakened natural immunity upon HCV infection, preferentially leading to failure of HCV-infected cell clearance [41].

Finally, our follow-up survey of the HCV persistence group indicated that increased T_H1 cell percentages were associated with accelerated progression of liver fibrosis, whereas T_C1 and NK cell percentages were inversely associated with progression (Table 4). In accordance with preceding studies [26,28,42], this study demonstrates that T_H1 immunity plays a vital role in HCV-related fibrosis progression. In the liver as well as peripheral blood of individuals with chronic HCV infection, T_H1 cells may enhance CTL response and macrophage activation by producing cytokines, such as IL-2, IFN-γ, and tumor necrosis factor-α, thereby facilitating the necro-inflammatory process of hepatitis C [26,42]. By contrast, increased T_C1 cell percentages in total CD8 T cells were associated with slower progression of fibrosis—new findings reported in this study. T_C1 cells express a chemokine receptor, CXCR3, which is required for migration to the HCV-infected liver [22], and we inferred that the increased T_C1 fraction includes HCV-specific CD8 T cells. Several studies have demonstrated relationships between higher numbers of circulating as well as intrahepatic HCV-specific CD8 T cells and lesser degrees of liver fibrosis during chronic HCV infection [43–46]. A plausible explanation is that HCV-specific CD8 T cells might control the virus without exerting cytotoxic effects on hepatocytes [46]. Alternatively, a population of CD8 T cells secreting an antifibrotic cytokine, IL-10, may be implicated in attenuation of hepatocyte killing and protection against liver injury [45,47].

A limitation of this study is that we examined clinical and immunologic data only from peripheral blood. Intrahepatic lymphocytes are assumed to have features distinct from those in peripheral blood [48]. Also, our comparison of lymphocyte subsets among study groups was cross-sectional, making it difficult to identify immunologic factors responsible for persistent HCV infection.

In conclusion, this study identified immunologic characteristics associated with HCV infection in a Japanese population and also indicated that peripheral T_H1, T_C1, and NK cell subsets will be useful for predicting progression of hepatitis in persistently HCV-infected patients and consequent development of hepatocellular carcinomas.

Acknowledgments

The Radiation Effects Research Foundation (RERF), Hiroshima and Nagasaki, Japan, is a private, nonprofit foundation funded by the Japanese Ministry of Health, Labor, and Welfare and the U.S. Department of Energy, the latter in part through the National Academy of Sciences. This research was based on RERF Research Protocols 3-09, 4-02, 2-00, and 9-92 and was supported in part by the U.S. National Institute of Allergy and Infectious Diseases (NIAID Contract HHSN272200900059C).

Appendix. Supplementary data

Supplementary data associated with this article can be found, in the online version, at doi:10.1016/j.humimm.2011.05.029.

References

[1] Shepard CW, Finelli L, Alter MJ. Global epidemiology of hepatitis C virus infection. Lancet Infect Dis 2005;5:558–67.
[2] Fung J, Lai CL, Yuen MF. Hepatitis B and C virus-related carcinogenesis. Clin Microbiol Infect 2009;15:964–70.
[3] Post J, Ratnarajah S, Lloyd AR. Immunological determinants of the outcomes from primary hepatitis C infection. Cell Mol Life Sci 2009;66:733–56.
[4] Sklan EH, Charuworn P, Pang PS, Glenn JS. Mechanisms of HCV survival in the host. Nat. Rev Gastroenterol Hepatol 2009;6:217–27.
[5] Crotta S, Stilla A, Wack A, D'Andrea A, Nuti S, D'Oro U, et al. Inhibition of natural killer cells through engagement of CD81 by the major hepatitis C virus envelope protein. J Exp Med 2002;195:35–41.
[6] Nattermann J, Nischalke HD, Hofmeister V, Ahlenstiel G, Zimmermann H, Leifeld L, et al. The HLA-A2 restricted T cell epitope HCV core 35-44 stabilizes HLA-E expression and inhibits cytolysis mediated by natural killer cells. Am J Pathol 2005;166:443–53.
[7] Piasecki BA, Lewis JD, Reddy KR, Bellamy SL, Porter SB, Weinrieb RM, et al. Influence of alcohol use, race, and viral coinfections on spontaneous HCV clearance in a US veteran population. Hepatology 2004;40:892–9.
[8] Stämpfli MR, Anderson GP. How cigarette smoke skews immune responses to promote infection, lung disease and cancer. Nat Rev Immunol 2009;9:377–84.
[9] Kusunoki Y, Hayashi T. Long-lasting alterations of the immune system by ionizing radiation exposure: implications for disease development among atomic bomb survivors. Int J Radiat Biol 2008;84:1–14.
[10] Ellenberg JH, Nelson KB. Sample selection and the natural history of disease. Studies of febrile seizures. JAMA 1980;243:1337–40.
[11] Beebe GW, Fujisawa H, Yamasaki M. Adult Health Study Reference Papers, A: Selection of the Sample, and B: Characteristics of the Sample. Technical Report 10-60. Hiroshima: Atomic Bomb Casualty Comission; 1960.
[12] Fujiwara S, Kusumi S, Cologne J, Akahoshi M, Kodama K, Yoshizawa H. Prevalence of anti-hepatitis C virus antibody and chronic liver disease among atomic bomb survivors. Radiat Res 2000;154:12–9.
[13] Ono E, Shiratori Y, Okudaira T, Imamura M, Teratani T, Kanai F, et al. Platelet count reflects stage of chronic hepatitis C. Hepatol Res 1999;15:192–200.
[14] Pohl A, Behling C, Oliver D, Kilani M, Monson P, Hassanein T. Serum aminotransferase levels and platelet counts as predictors of degree of fibrosis in chronic hepatitis C virus infection. Am J Gastroenterol 2001;96:3142–6.
[15] Coverdale SA, Samarasinghe DA, Lin R, Kench J, Byth K, Khan MH, et al. Changes in antipyrine clearance and platelet count, but not conventional liver tests, correlate with fibrotic change in chronic hepatitis C: value for predicting fibrotic progression. Am J Gastroenterol 2003;98:1384–90.
[16] Moriyama M, Matsumura H, Aoki H, Shimizu T, Nakai K, Saito T, et al. Long-term outcome, with monitoring of platelet counts, in patients with chronic hepatitis C and liver cirrhosis after interferon therapy. Intervirology 2003;46:296–307.
[17] Kawasaki T, Takeshita A, Souda K, Kobayashi Y, Kikuyama M, Suzuki F, et al. Serum thrombopoietin levels in patients with chronic hepatitis and liver cirrhosis. Am J Gastroenterol 1999;94:1918–22.
[18] Olariu M, Olariu C, Olteanu D. Thrombocytopenia in chronic hepatitis C. J Gastrointest Liver Dis 2010;19:381–5.
[19] Cullings HM, Fujita S, Funamoto S, Grant EJ, Kerr GD, Preston DL. Dose estimation for atomic bomb survivor studies: its evolution and present status. Radiat Res 2006;166:219–54.
[20] Sallusto F, Lenig D, Mackay CR, Lanzavecchia A. Flexible programs of chemokine receptor expression on human polarized T helper 1 and 2 lymphocytes. J Exp Med 1998;187:875–83.
[21] Cosmi L, Annunziato F, Galli MIG, Maggi RME, Nagata K, Romagnani S. CRTH2 is the most reliable marker for the detection of circulating human type 2 Th and type 2 T cytotoxic cells in health and disease. Eur J Immunol 2000;30:2972–9.

[22] Larrubia JR, Calvino M, Benito S, Sanz-de-Villalobos E, Perna C, Perez-Hornedo J, et al. The role of CCR5/CXCR3 expressing CD8+ cells in liver damage and viral control during persistent hepatitis C virus infection. J Hepatol 2007;47:632–41.
[23] Yamaoka M, Kusunoki Y, Kasagi F, Hayashi T, Nakachi K, Kyoizumi S. Decreases in percentages of naïve CD4 and CD8 T cells and increases in percentages of memory CD8 T-cell subsets in the peripheral blood lymphocyte populations of A-bomb survivors. Radiat Res 2004;161:290–8.
[24] Armitage P, Berry G, Matthews JNS. Statistical Methods in Medical Research (4th ed). Oxford: Blackwell Scientific; 2002.
[25] Hayashi T, Morishita Y, Kubo Y, Kusunoki Y, Hayashi I, Kasagi F, et al. Long-term effects of radiation dose on inflammatory markers in atomic bomb survivors. Am J Med 2005;118:83–6.
[26] Napoli J, Bishop GA, McGuinness PH, Painter DM, McCaughan GW. Progressive liver injury in chronic hepatitis C infection correlates with increased intrahepatic expression of Th1-associated cytokines. Hepatology 1996;24:759–65.
[27] Bergamini A, Bolacchi F, Cerasari G, Carvelli C, Faggioli E, Cepparulo M, et al. Lack of evidence for the Th2 predominance in patients with chronic hepatitis C. Clin Exp Immunol 2001;123:451–8.
[28] Sobue S, Nomura T, Ishikawa T, Ito S, Saso K, Ohara H, et al. Th1/Th2 cytokine profiles and their relationship to clinical features in patients with chronic hepatitis C virus infection. J Gastroenterol 2001;36:544–51.
[29] Gigi E, Raptopoulou-Gigi M, Kalogeridis A, Masiou S, Orphanou E, Vrettou E, et al. Cytokine mRNA expression in hepatitis C virus infection: TH1 predominance in patients with chronic hepatitis C and TH1–TH2 cytokine profile in subjects with self-limited disease. J Viral Hepat 2008;15:145–54.
[30] Reiser M, Marousis CG, Nelson DR, Lauer G, González-Peralta RP, Davis GL, et al. Serum interleukin 4 and interleukin 10 levels in patients with chronic hepatitis C virus infection. J Hepatol 1997;26:471–8.
[31] Fan XG, Liu WE, Li CZ, Wang ZC, Luo LX, Tan DM, et al. Circulating Th1 and Th2 cytokines in patients with hepatitis C virus infection. Mediat Inflamm 1998;7:295–7.
[32] Abayli B, Canataroğlu A, Akkiz H. Serum profile of T helper 1 and T helper 2 cytokines in patients with chronic hepatitis C virus infection. Turk J Gastroenterol 2003;14:7–11.
[33] Cacciarelli TV, Martinez OM, Gish RG, Villanueva JC, Krams SM. Immunoregulatory cytokines in chronic hepatitis C virus infection: pre- and posttreatment with interferon alfa. Hepatology 1996;24:6–9.
[34] Kakumu S, Okumura A, Ishikawa T, Yano M, Enomoto A, Nishimura H, et al. Serum levels of IL-10, IL-15 and soluble tumour necrosis factor-alpha (TNF-alpha) receptors in type C chronic liver disease. Clin Exp Immunol 1997;109:458–63.
[35] Anthony DD, Post AB, Valdez H, Peterson DL, Murphy M, Heeger PS. ELISPOT analysis of hepatitis C virus protein-specific IFN-gamma-producing peripheral blood lymphocytes in infected humans with and without cirrhosis. Clin Immunol 2001;99:232–40.
[36] Chan TM, Ho SK, Lai CL, Cheng IK, Lai KN. Lymphocyte subsets in renal allograft recipients with chronic hepatitis C virus infection. Nephrol Dial Transplant 1999;14:717–22.
[37] Chang KM, Thimme R, Melpolder JJ, Oldach D, Pemberton J, Moorhead-Loudis J, et al. Differential CD4(+) and CD8(+) T-cell responsiveness in hepatitis C virus infection. Hepatology 2001;33:267–76.
[38] Pár G, Rukavina D, Podack ER, Horányi M, Szekeres-Barthó J, Hegedüs G, et al. Decrease in CD3-negative-CD8dim(+) and Vdelta2/Vgamma9 TcR+ peripheral blood lymphocyte counts, low perforin expression and the impairment of natural killer cell activity is associated with chronic hepatitis C virus infection. J Hepatol 2002;37:514–22.
[39] Morishima C, Paschal DM, Wang CC, Yoshihara CS, Wood BL, Yeo AE, et al. Decreased NK cell frequency in chronic hepatitis C does not affect ex vivo cytolytic killing. Hepatology 2006;43:573–80.
[40] Andrews DM, Estcourt MJ, Andoniou CE, Wikstrom ME, Khong A, Voigt V, et al. Innate immunity defines the capacity of antiviral T cells to limit persistent infection. J Exp Med 2010;207:1333–43.
[41] Golden-Mason L, Cox AL, Randall JA, Cheng L, Rosen HR. Increased natural killer cell cytotoxicity and NKp30 expression protects against hepatitis C virus infection in high-risk individuals and inhibits replication in vitro. Hepatology 2010;52:1581–9.
[42] Moura AS, Carmo RA, Teixeira AL, Leite VH, Rocha MO. Soluble inflammatory markers as predictors of liver histological changes in patients with chronic hepatitis C virus infection. Eur J Clin Microbiol Infect Dis 2010;29:1153–61.
[43] Sreenarasimhaiah J, Jaramillo A, Crippin J, Lisker-Melman M, Chapman WC, Mohanakumar T. Lack of optimal T-cell reactivity against the hepatitis C virus is associated with the development of fibrosis/cirrhosis during chronic hepatitis. Hum Immunol 2003;64:224–30.
[44] Cardoso EM, Duarte MA, Ribeiro E, Rodrigues P, Hultcrantz R, Sampaio P, et al. A study of some hepatic immunological markers, iron load and virus genotype in chronic hepatitis C. J Hepatol 2004;41:319–26.
[45] Abel M, Sène D, Pol S, Bourlière M, Poynard T, Charlotte F, et al. Intrahepatic virus-specific IL-10-producing CD8 T cells prevent liver damage during chronic hepatitis C virus infection. Hepatology 2006;44:1607–16.
[46] Bonilla N, Barget N, Andrieu M, Roulot D, Letoumelin P, Grando V, et al. Interferon gamma-secreting HCV-specific CD8+ T cells in the liver of patients with chronic C hepatitis: relation to liver fibrosis—ANRS HC EP07 study. J Viral Hepatol 2006;13:474–81.
[47] Accapezzato D, Francavilla V, Paroli M, Casciaro M, Chircu LV, Cividini A, et al. Hepatic expansion of a virus-specific regulatory CD8(+) T cell population in chronic hepatitis C virus infection. J Clin Invest 2004;113:963–72.
[48] Grabowska AM, Lechner F, Klenerman P, Tighe PJ, Ryder S, Ball JK, et al. Direct ex vivo comparison of the breadth and specificity of the T cells in the liver and peripheral blood of patients with chronic HCV infection. Eur J Immunol 2001;31:2388–94.

Mutation Research 721 (2011) 101–107

Contents lists available at ScienceDirect

Mutation Research/Genetic Toxicology and Environmental Mutagenesis

journal homepage: www.elsevier.com/locate/gentox
Community address: www.elsevier.com/locate/mutres

Easy detection of GFP-positive mutants following forward mutations at specific gene locus in cultured human cells

Asao Noda[a,*], Yuko Hirai[a], Yoshiaki Kodama[a], Warren W. Kretzschmar[a], Kanya Hamasaki[a], Yoichiro Kusunoki[b], Hiroshi Mitani[c], Harry M. Cullings[d], Nori Nakamura[a]

[a] Department of Genetics, Radiation Effects Research Foundation, 5-2 Hijiyama Park, Minami-Ku, Hiroshima 732-0815, Japan
[b] Departments of Radiobiology and Molecular Epidemiology, Radiation Effects Research Foundation, 5-2 Hijiyama Park, Minami-Ku, Hiroshima 732-0815, Japan
[c] Department of Integrated Biosciences, Graduate School of Frontier Sciences, The University of Tokyo, Kashiwa-no-ha 5-1-5, Kashiwa, Chiba 277-8572, Japan
[d] Department of Statistics, Radiation Effects Research Foundation, 5-2 Hijiyama Park, Minami-Ku, Hiroshima 732-0815, Japan

ARTICLE INFO

Article history:
Received 5 October 2010
Received in revised form
19 November 2010
Accepted 29 December 2010
Available online 6 January 2011

Keywords:
Radiation
Tet repressor
Tet operator
GFP
HPRT

ABSTRACT

We have generated a new mutation assay system using HT1080 human fibrosarcoma cells, which consists of a combination of tetracycline-operator dependent *GFP* gene (*TetO-EGFP*) and tetracycline repressor (*TetR*) genes, where the expression of *GFP* gene is under strict control of TetR protein, and the *TetR* gene is located within the endogenous *HPRT* gene. In this system, any inactivating mutation at the *TetR* gene or large deletions including the gene itself results in high expression of *GFP* gene (>200-fold increase) in the cells, which can be readily scored not only by a flow cytometer but also under a fluorescent microscope. With this new cell line, we show that the spontaneous mutation rate at the *TetR* locus was $2.8–3.4 \times 10^{-6}$/cell division, slightly lower than the rate at the endogenous *HPRT* gene of HT1080 cells, and has a dose response to X rays as a mutagen. We also isolated variant clones with elevated spontaneous mutation rate (i.e., genetically unstable cells) following X irradiation. Spontaneous GFP-positive mutants were predominantly base-change mutations at the *TetR* gene while those obtained after X irradiation often contained large deletions which spanned up to 6 Mb. The results indicate that the bacterial TetR/TetO regulatory units work extremely well as a mutation detection system in human cells, and any part of the human genome may be tested for mutation sensitivity following targeted insertion of the *TetR* gene in a stably expressing gene.

1. Introduction

Quite a large number of chemicals are newly produced every year and it is desired that genotoxic chemicals are effectively excluded from our living environment as they are potentially carcinogenic. Such an effort is important for living in a safe environment. Accordingly, screening of a large number of environmental mutagens has been conducted using bacteria and cultured mammalian cells [1,2].

In cultured mammalian cells, mutation detection systems use primarily genes involved in salvage pathways of nucleic acid synthesis (the genes are non-essential for cell survival); namely, *HPRT* and *TK* genes. Normal cells die in the presence of cytotoxic analogues (6-thioguanine or trifluorothymidine, respectively) by incorporating them into nucleic acids, while mutant cells deficient in the enzyme activity cannot utilize the analogue and survive as they use *de novo* pathways for the nucleic acid synthesis [3,4]. In those systems, cells treated with test chemicals have to be subcultured for a few days to nearly 1 week for the full expression of the mutant phenotype before being subjected to colony formation in selective media, a step that takes an additional 1–2 weeks. Thus, a total of 2–3 weeks are required for one set of experiments.

There are also *in vivo* systems which utilize naturally available mutant alleles of mice; namely, pink eye unstable (p^{un}) in retina and coat hair [5], and *Dlb-1* in colon [6]. Expression of those genes is restricted to specific tissues, however, which limits the usefulness of the systems as a tool for screening environmental mutagens. Other *in vivo* systems utilize *Hprt*, and animals heterozygous for the endogenous *Tk* and *Aprt* genes as reporters. All share the limitation of only being performed in a small number of cell types, such as T lymphocytes and skin fibroblasts.

More recently, developments of molecular biology techniques have added new options to create systems with foreign reporter genes for mutagenesis studies. One class of such systems consists of a gene originating from prokaryotes that is inserted into the mammalian genome. Following mutagen treatment, DNA is recovered and mutations are quantified and analyzed in *Escherichia coli* [7]. Several different strains of transgenic animals using such a

* Corresponding author. Tel.: +81 82 261 3131; fax: +81 82 263 7279.
E-mail addresses: asnoda@rerf.or.jp, gk7a-nd@asahi-net.or.jp (A. Noda).

1383-5718/$ – see front matter © 2011 Elsevier B.V. All rights reserved.
doi:10.1016/j.mrgentox.2010.12.010

system have also been produced [8]. The second class is a mutation detection system in which mutations are more easily detected *in situ* in genetically altered cells which carry a transgene, most frequently green fluorescence protein (*GFP*) gene. In such a system, the reporter gene is set as not to express under normal conditions, but to express following mutagenesis. For example, in a system consisting of a tandem array of two *GFP* genes each of which contains mutations at different sites, gene conversion-type events primarily give rise to an intact *GFP* gene [9–14]. In another system consisting of *GFP* genes which were purposely set as out of reading frame by an insertion of micro-repeat sequences at its 5′ side, deletion of restricted numbers of bases can make the gene in frame and the cells will fluoresce [15,16]. Transgenic animals are also created [10]. The major constraint of those assays is that only specific types of mutational events are detectable. And obviously, it is not possible to detect large deletions including the reporter gene and the neighboring segments of DNA (e.g., 1 Mb deletions), frequent events following exposure to ionizing radiations.

Therefore, for detection of both base substitutions and large deletions, a reversion system cannot satisfy the conditions but a component of a forward mutation system needs to be included. We propose that a possible system is a compound two-gene system comprised suppressor and effector genes. Dobrovolsky et al. [17] previously used a compound system consisting of tetracycline-inducible repressor (*TetR*) gene and *GFP* gene, the latter is under the control of tetracycline-operator (*TetO-GFP*). They reported, however, that the suppressive function of the *TetR* gene was not effective enough and it was difficult to distinguish mutants from cells with intermediate levels of GFP expression, probably due to multiple copies of the integrated *GFP* genes and/or epigenetic modification of the *TetR* gene. Consequently, the system is not easy to use as a mutation-screening system. In the present study, we have overcome the problems using a single copy integration of *GFP* gene and targeted insertion of the *TetR* gene into intron 3 of the endogenous *HPRT* gene, which is known to be ubiquitously expressed. With the new system, it is now possible to measure any inactivating mutations (forward mutations) in the target *TetR* gene by means of flow-cytometry. We can measure not only spontaneous mutation rates, but also mutagenic effects of large and small doses of ionizing radiation. Applications of the system to an *in vivo* system will also be discussed.

2. Materials and methods

2.1. Cells and culture conditions

Human fibrosarcoma cell line HT1080 (ATCC No. CCL121), carrying a nearly normal karyotype (44+XY; [18]), was used throughout the study. The cells were maintained under standard culture conditions (MEM with Earl's salts supplemented with 10% FCS), and antibiotics G418 (400 μg/ml), blasticidin (5 μg/ml), or tetracycline (1 μg/ml), was added when necessary. To isolate HPRT proficient or deficient cells, HAT (1 × HAT) or 6TG (2.5 μg/ml)-containing medium was used for the respective selection. X-irradiation was carried out with a Shimadzu X-irradiator (220 kV, 8 mA with 0.5 mm Al and 0.3 mm Cu filters) with a dose rate of about 0.34 Gy/min. For flow-cytometric analyses, cells were treated with trypsin–EDTA, and were suspended in PBS containing 1% FCS at about 10^6 cells/ml. Samples were analyzed by a flow cytometer or a cell sorter (FACScan; Becton, NJ or JSAN; Bay Bioscience, Kobe) by gating single cells.

2.2. Plasmid construction and gene targeting (Supplementary figures)

2.2.1. Tetracycline operator (TetO)-driven EGFP vector

EGFP gene fragment (0.8 kb) was excised from plasmid pEGFP-C1 (Clonetech) by *Eco*47III and *Sma*I digestion, and ligated with *Eco*RV digested pcDNA4/TO (Invitrogen) which carries CMV promoter in conjunction with tandem duplicated Tet operator sequences (2 × TetO). The resulting plasmid, pTetO-GFP#16, was linearized by partial digestion with *Hin*dIII, and ligated with a *Hin*dIII-digested bsr fragment (0.5 kb) from pSV2bsr (Funakoshi) to make plasmid pTetO-GFPbsr#45. The plasmid was then digested with *Apa*I and recircularized to remove unnecessary sequences (*Xho*I site) flanked with the 3′ side of bsr. The resulting plasmid (pTetO-GFPbsr#45-(-Xho)#15) was digested with *Xho*I, filled-in and religated to make GFP-bsr fusion gene (plasmid pTetO-EGFPbsr#1). The plasmid was linearized by digestion with *Ssp*I, and electroporated into HT1080 cells using standard pulse settings for adherent cells (25 μF, 1000 V). Colonies resistant to blasticidin were recovered and propagated. Intensity of GFP fluorescence was measured in order to select clones that exhibit strong and uniform GFP expression among the cells in that clone.

2.2.2. HPRT gene targeting vector

A 8.4 kb of genomic DNA fragment containing human *HPRT* exons 2 and 3 (left arm of the targeting vector) was isolated from the human BAC clone (bWXD187, AC004387) by *Eco*RI digestion [18] and was inserted into the *Eco*RI site of the pBS(SKII) plasmid. The resulting plasmid was digested with *Eco*RV, and ligated with blunted DNA fragment containing a CMV promoter-Tet repressor (*TetR*) gene unit [a 2.3 kb of *Mlu*I fragment from the plasmid pcDNA6/TR (Invitrogen), where both *Mlu*I ends were filled-in], resulting in the plasmid p8.4-6TR#2. Next, 2.3 kb of DNA fragment (right arm of targeting vector), derived from *Eco*RI-digest of human *HPRT* intron 3, was inserted into *Eco*RI digested pBS(SKII) to make plasmid pBS2.3#3. Then 1.2 kb of the loxP-neo gene fragment was excised from pBS-MCneo [18] by *Sma*I and *Hin*cII digestion, and ligated with *Sma*I-digested pBS2.3#3 to make plasmid p2.3neo#1. To exclude cells that have undergone untargeted integration of the vector (random insertion in the genome), a 1.1 kb of *DTA* gene fragment which encodes diphtheria toxin [19] and is derived from *Eco*RV and *Hin*cII digestion of pBS-MC1DTA, was also inserted into blunted-*Sal*I site of p2.3neo#1 to give the plasmid p2.3neoDTA#2. Then, a 4.6 kb of neo-2.3kb-DTA fragment was excised from p2.3neoDTA#2 by *Sma*I and *Apa*I digestion, filled-in, and then inserted into blunted-*Sal*I site of the plasmid p8.4-6TR#2 to give the targeting plasmid, pHPRT-6TRtarget#6.

2.2.3. Targeted integration of CMV TetR-floxed neo gene fragment into endogenous HPRT gene locus

The 15.4 kb of the targeting fragment from the vector (HPRT-6TR fragment) was isolated with *Bss*HII digestion, and electroporated into the selected cell clones obtained from the above-mentioned step (2.2.1), whose GFP expression was highest. Among the G418 resistant clones recovered, those which underwent correct integration of the HPRT-6TR fragment into endogenous *HPRT* gene through homologous recombination were identified by PCR and Southern analyses (Fig. 1). As expected, those clones showed no *GFP* gene expression through silencing by TetR protein.

2.3. Detection of mutant cells

Any loss-of-function mutation at the *TetR* gene located in the *HPRT* locus, irrespective of point mutations or deletions encompassing the integrated *TetR* sequences, releases the *GFP* gene expression from silencing. Adding tetracycline (1 μg/ml) into the culture media can simulate this release. Presumed *TetR* mutant cells were defined as having GFP levels equivalent to those of tetracycline-treated cells. This equivalency of GFP expression was confirmed by flow cytometry. We defined mutants as cells displaying elevated levels of fluorescence intensity of GFP by at least 200-fold compared with the level of autofluorescence of wild-type or untreated cells (Fig. 2A)

2.4. Mutation assay

Clonal cell populations propagated from a single cell were grown up to 4.5×10^7 cells, and were then cryopreserved in 10 ampoules (4.5×10^6 cells each). Each ampoule was thawed and used for each set of mutagenesis experiments so that the background mutation frequency should remain low and constant. The frequency of GFP-positive mutant cells was measured by a flow cytometer (FACScan, Becton-Dickinson) by screening at least 10^6 cells per sample. In low dose experiments (Fig. 4C), 10^7 cells were subjected for each measurement.

2.5. Isolations and characterizations of mutant cells by multiplex PCR

Mutant cells that arose in the cultures of unirradiated or irradiated cells were detected and isolated with a desk-top cell sorter, JSAN. Each mutant was isolated and propagated up to 2×10^6 cells, and their genomic DNA was extracted. Multiplex PCR (Qiagen kit) was carried out to amplify *HPRT* exons 1–9 as well as integrated *TetR* gene in a single tube. Primers used are: HPRT exon 1 (TGGGACGTCTGGTCCAAGGATTCA, CCGAACCCGGGAAACTGGCCGCCC), exon 2 (CACCTAAATTTCTCTGATAGACTAAGG, GATACTAAGTAATTAGTAAGGCC), exon 3 (GTGGAAGTTTAATGACTAAGAG, GTATATATCCTCCAAGGTGACTAG), exon 4 (GCTATGGATATTAGCTAGCTAAC, GCTTCCAAGGGTTAAATAACCCA), exon 5 (AGCATCTAAAAACAAGAGTTTGG, AACTGATGCAGAGGAATTTCTCTC), exon 6 (GATTTTGGTGAGAATTACTGTGCTG, CACTTAATCCCCCTTCAAATGAG), exons 7+8 (ACCAAGTGCCTTGTCTGTAGTGTC, TCCTAAATCTTCCTCAACCATGTTC), exon 9 (ACTAATGTGATAGACTACTGC, GAACTGCTGACAAAGATTCACTG), TetR (AGGGCGAATTGATATGTCTAGA, GCTGCAATAAACAAGTTCTGCT) [20].

For genome walking with STS PCR, we set STS primers at about 1 Mb intervals from both sides of the *HPRT* gene locus, and multiplex PCR with different combinations of 15 STS sites was carried out to reveal the deletion size of the DNA sequences around *HPRT* (*TetR*) gene locus. For those mutants with no evidence of deletion of

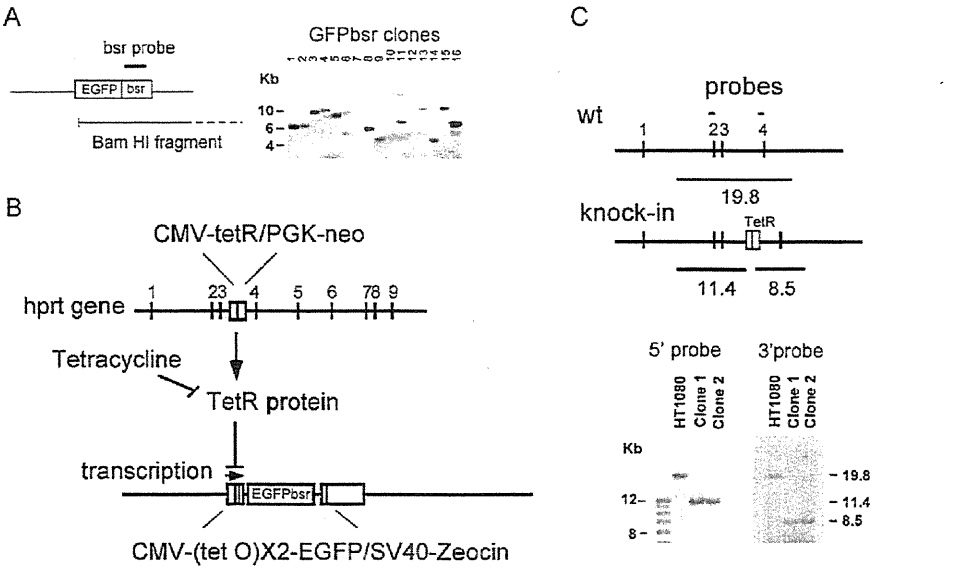

Fig. 1. Generation of GFP transgenic/TetR knock-in HT1080 cells. (A) Integration of a single copy of a vector carrying the TetO-EGFPbsr sequence. The left picture indicates locations of the bsr probe and *Bam*HI site, and the right panel shows the results of Southern blots of 16 transfectants. (B) Diagram illustrating the intracellular system in which GFP transcription is induced by inactivation of *TetR* gene which was inserted in intron 3 of *HPRT* gene by targeted insertion, or by inhibition of TetR protein with tetracycline. (C) Verification of targeted integration of *TetR* gene. DNA from the candidate clones were digested with *StuI* and hybridized with 5′ or 3′ probes, respectively. Locations of the probes and fragments to be detected are indicated. In wild-type cells both probes detected the 19.8 kb band, while in knock-in cells 5′ and 3′ probes detected the 11.4 and 8.5 kb bands, respectively.

any *HPRT* exon, *TetR* gene was amplified by PCR and sequenced to determine the site of point mutations.

2.6. Measurements of mutant frequency and estimation of spontaneous mutation rate

One ampoule was thawed and 4×10^6 cells were used to initiate a culture. Every 3–4 days, cell number as well as mutant cell frequency were determined and 4×10^6 cells were taken anew to continue the culture. The experiments were repeated twice (this is termed as "large-scale inoculation and short-term culture").

The spontaneous mutation rate was calculated as reported by Nadas et al. [21,22] and Foster [23]. In brief, we assumed that only one of the two daughter cells becomes mutant following a spontaneous mutation in a cell cycle because most of the spontaneous mutations are base-change mutations and hence would affect only one strand of the DNA double strands. Assume that there are m mutant cells preexisting in a

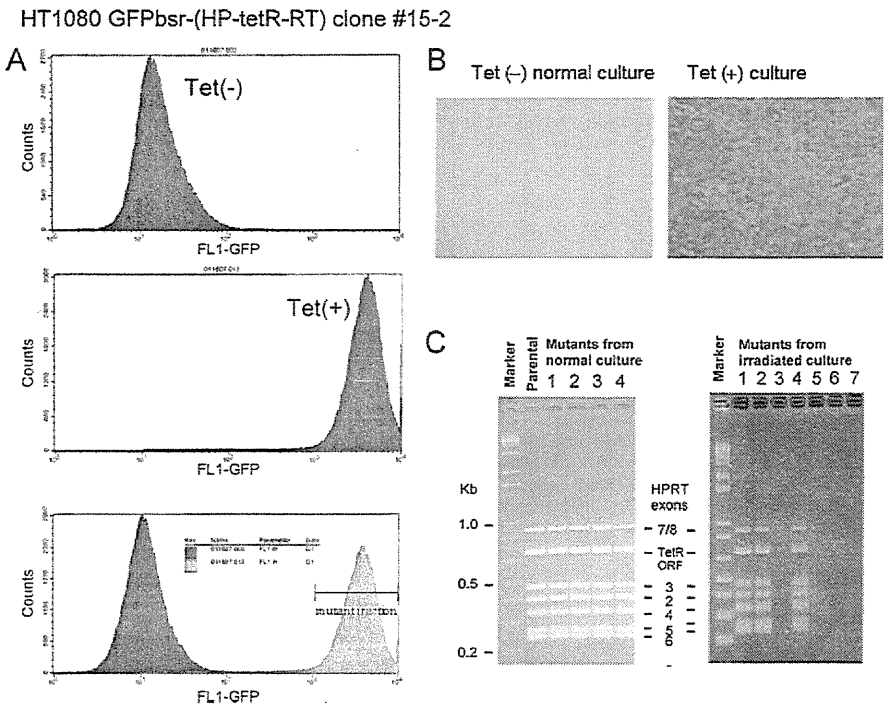

Fig. 2. Tet On/Off system verifications and analyses of spontaneous and radiation-related mutants. (A) Flow cytometric analyses of HT1080 cells bearing the TetR/TetO-GFP system cultured overnight in the absence [Tet(−), upper panel] or the presence of tetracycline [Tet(+), middle panel]. The lower panel indicates the window for mutant detection (the mean fluorescent intensity is >250-fold higher than in normal cells). (B) Two representative views under fluorescent microscopy (×100). (C) Molecular analyses of mutant clones for the presence or absence of *HPRT* exons and *TetR* gene by multiplex PCR. All spontaneous mutants retained the 7 exons whereas four out of seven mutants recovered after radiation exposure had lost all of them.

starting population consisting of n_0 cells and the population reaches n_1 at the end of the culture, which took a generations; namely, $n_1 = n_0 \times 2^{a-1}$.

In such a growing cell population, new mutants arise in proportion to the number of cells that divide. Thus, at ith generation, the number of cells that divide is $n_0 \times 2^{i-1}$, and hence the number of new mutants is $p(n_0 \times 2^{i-1})$, where p stands for the spontaneous mutation rate. Since these mutants continue to divide until the population reaches ath generation, the number of mutants increases by $2^{(a-i)}$. That is, each generation equally contributes to produce spontaneous mutants by $p(n_0 \times 2^{i-1}) \times 2^{(a-i)} = p(n_0 \times 2^{a-1})$, and hence the total number of new mutants is $p(n_0 \times 2^{a-1}) \times a$ when the cell number reaches n_1.

In practice, let the mutant frequency measured at the start and the end of the culture be Mf_0 and Mf_1. Mf_1 is described as a function of the preexisting mutants plus new mutants that arose during this culture period, namely, $Mf_1 = m/n_0 + [p(n_0 \times 2^{a-1}) \times a/(n_0 \times 2^{a-1})]$. Since $Mf_0 = m/n_0$, the net increase of the mutant frequency is;

$$Mf_1 - Mf_0 = \left[\frac{p(n_0 \times 2^{a-1}) \times a}{(n_0 \times 2^{a-1})}\right] = pa \quad (1)$$

The classical Luria Delbrück fluctuation test was also conducted as previously reported except that, instead of using colony formation assay, mutant cell frequency was determined by flow cytometry. In brief, cells were inoculated at a low density, and 20–100 individual colonies were randomly isolated. Each colony was propagated to 2×10^6 cells, and the number of mutants in these cultures was determined. Mutation rates were calculated as follows:

$$r = aN \times \ln(NCa) \quad (2)$$

where r is the average number of mutants in each of the separately propagated cultures; a is the mutation rate; N is the number of cells in the expanded populations (2×10^6 in this case), and C is the number of clones examined [18,24].

For radiation mutagenesis experiments, 4×10^6 cell-aliquots were irradiated for each dose level, cultured for 6 days for the full expression of the mutant phenotype, and subjected to flow cytometric analysis to determine the mutant frequency.

2.7. Isolation of cell clones exhibiting genomic instability after X-irradiation

Three million cells were irradiated with 4 Gy, followed by a 5-day culture, trypsinized, and seeded at low densities. Then 400 individual colonies were randomly isolated and individually cultured in each well of 96-well plates until they reached confluence (about 2×10^4 cells/well). The number of mutants in individual wells was then counted under a fluorescent microscope. Wells containing more than 10 mutants were selected as candidate clones possibly harboring cells with genomic instability. Each clone was further propagated and examined for estimation of mutation rate with the "large-scale inoculation and short-term culture" method as well as the fluctuation test [24].

3. Results

3.1. Generation of cells bearing TetO-GFP gene which is under strict control by TetR gene

As mentioned in Section 1, the present study was aimed at creating a model system using a human cell line in which any inactivating mutations at *TetR*, including surrounding *HPRT* locus may be detected as GFP-positive cells. For this purpose, we used a compound system consisting of a combination of *TetR* and *TetO-GFP* genes.

In the first set of the experiments, cells were transfected with TetO-GFP-containing plasmids by chemical lipofection. However, all the blasticidin-resistant clones were found to contain multiple copies of the plasmid. Since we did not feel that this is a critical problem, we used those cells for targeted integration of *TetR* gene into the endogenous *HPRT* locus. About 30 candidate clones were isolated, but all of them showed variable frequencies of GFP-positive "mutant" cells at 10^{-4} to 10^{-3}, which seemed to be too high to be caused by true mutations. We speculated that this was probably because a single-copy *TetR* gene was insufficient to fully silence the expression of multicopied *TetO-GFP* genes, and decided to change the strategy to generate cells consisting of single copy integrations for both *TetR* and *TetO-GFP* genes.

For this purpose, we switched to use an electroporation technique in isolating GFP-positive and blasticidin-resistant clones, and found that the majority of the transfectants (~75%) contained a single copy of *TetO-GFP* gene (Fig. 1A). Subsequently, we isolated two clones (#3 and #15; Fig. 1A), which showed the brightest fluorescence intensity and carried a single copy of the gene, and used them as recipients for the second-step, targeted integration of the *TetR* gene into intron 3 of the *HPRT* gene also by electroporation. Among tens of thousands of G418 resistant colonies recovered, a few clones could be isolated which had undergone correct integrations of the *TetR* gene (Fig. 1B and C). We found that all the clones that had correct integration of *TetR* gene in the endogenous *HPRT* gene exhibited highly stable suppression of the *TetO-GFP* gene activity. It is noted that, although the *TetR* gene was integrated in a large intron 3, the normal function of the *HPRT* gene was destroyed and the cells became deficient in the HPRT activity (i.e., resistant to 6TG).

3.2. Flow cytometric analyses of the GFP-positive mutants

A high level of suppression of *TetO-GFP* gene activity by the expression of *TetR* gene was evident since, under normal culture conditions, no mutants were seen in most of the cell populations consisting of 5×10^5 cells, where each population originated from single cells. Further, the suppression was so profound that the expression level of GFP protein was increased by more than 200-fold upon inactivation of the TetR protein following treatment of the cells with tetracycline for overnight (*cf.* tet(−) and tet(+) panels in Fig. 2A). Since the lower limit of the fluorescence level specified for the GFP-positive cells is higher than the upper limit of the autofluorescence level of GFP-negative cells by one order of magnitude (Fig. 2A lower panel), we could clearly define the mutant window for GFP-positive cells as indicated with the cross-bar. It is noted that the normal cells are not completely negative with regard to the fluorescence emission but show a low level of autofluorescence. Namely, the level of autofluorescence was 1.5–2.0 times higher in the parental cells (#15-2) compared with those in the original HT1080 cells. We noted that culturing the cells in the presence of commercially available, antibiotics-free FCS could diminish the level of autofluorescence, but this was not essential for the measurements of mutant frequencies. GFP-positive and -negative cells can also be clearly distinguished under a fluorescent microscope (Fig. 2B).

Before conducting quantitative measurements of radiation dose response, expression time course for mutant phenotype was monitored following exposure of 4×10^6 cells to 4 Gy of X rays. The results are shown in Fig. 3A and B, and indicated that 6 days, or 3 PDs, were required before the *TetR*-gene mutants fully express the GFP-positive phenotype, indicating that the degradation, or dilution by cell division, of pre-existed TetR proteins would determine the latency.

3.3. Spontaneous and radiation-induced mutations

Spontaneous mutation rate was estimated following repeated measurements of the mutant cell frequencies by flow cytometry during subcultures of a large cell population (5×10^6 cells). The results indicate that the mutant frequency increases in proportion to the increase in the number of population doublings (Fig. 4A). As the net increase of the mutant frequency is about $17/5 \times 10^5$ cells (or 3.4×10^{-5}) at 20 population doublings, the mean increase is 0.17×10^{-5}/population doubling, which gives an estimate of the spontaneous mutation rate as 0.34×10^{-5}/cell division from Eq. (1).

Results of the X-ray mutagenesis are shown in Fig. 4B and C. It appears that the dose response curve showed upward curvature (Fig. 4B), with linear-quadratic regression statistically significant ($p = 0.03$ for the term $(X - 1.5)^2$). Eye fitting of the data indicates that about 1 Gy can give rise to double the background mutation frequency. Low dose experiments were also conducted in a separate set of experiments, in which a larger number of